

THESIS

MEMBRANE FLUIDITY OF RBL-2H3 CELLS TREATED WITH INSULIN AND BMOV  
USING TIME-CORRELATED SINGLE PHOTON COUNTING FLUORESCENCE  
ANISOTROPY

Submitted by

Chelsea Rene' Lenne Roan

Graduate Degree Program in Cell and Molecular Biology

In partial fulfillment of the requirements

For the Degree of Master of Science

Colorado State University

Fort Collins, Colorado

Summer 2013

Master's Committee:

Advisor: Deborah A. Roess

Co-Advisor: B. George Barisas

Debbie C. Crans

## ABSTRACT

### MEMBRANE FLUIDITY OF RBL-2H3 CELLS TREATED WITH INSULIN AND BMOV USING TIME-CORRELATED SINGLE PHOTON COUNTING FLUORESCENCE ANISOTROPY

Transition metal compounds have been shown to be insulin-enhancing but the mechanism of action has not been fully elucidated. With obesity, diabetes and other metabolic derangements increasing in developed countries, understanding the effects these compounds will better target drug therapy. Previous investigations have focused on vanadium and have studied the effects on protein-protein interactions in the insulin signaling pathway. In this paper, we propose that the mechanism of action may also include interactions with the plasma membrane. Lipids as bioactive molecules are on the horizon as the next great area of exploration in biochemistry and molecular biology. Within the insulin signaling pathway, the insulin receptor functions optimally in areas of specialized lipid packing that are characterized as small detergent insoluble regions enriched in sphingomyelin and cholesterol and termed lipid rafts. These lipid rafts are a subset of microdomains within the plasma membrane. Obesity and excess lipids have been shown to increase inflammation via increases in free fatty acids, cytokines, TNF- $\alpha$ , and reactive oxygen species resulting in the peroxidation of membrane lipids. We propose that one cause of insulin resistance, a failure of insulin receptors to respond to insulin, is due to disruption of the membrane lipids resulting in an increase in membrane fluidity. This disruption results in displacement of insulin receptors out of specialized lipid rafts. We propose that treatment with vanadium will result in an increase in membrane rigidity favoring lipid raft formation and

restoration of insulin receptors to a platform favoring optimal signaling. Time-correlated single photon counting fluorescence anisotropy was used to measure the membrane fluidity of RBL-2H3 cells treated with insulin and the vanadium compound bis(maltolato)oxovanadium(IV) (BMOV).

## ACKNOWLEDGEMENTS

I am grateful for the support of many who have made this endeavor possible. I would like to start by thanking Dr. Deb Roess and Dr. B. George Barisas who welcomed me into their lab as a naïve undergraduate student. You two have taught me more than science; you have demonstrated compassion for others, encouragement, and patience. Thank you for your friendship. I will miss you. To Dr. Debbie Crans, thank you for your enthusiasm. To my lab mates, thank you for the friendship, coffee and laughs throughout the years.

To Lori Williams in the Graduate School office, thank you for your friendship and for helping me navigate all of the hoops and paperwork.

To all of my family, the Roan's, the Wiik's, the Wilson's, the Lenne's, the Brakebill's, and to extended family cheering from afar, thank you. Without your love and support, I would not have been able to do this, and I do not take lightly the sacrifices you have made to help me reach my goals. Thank you for loving me and loving Jaxon during the long hours spent in the lab and in writing. Audrienne, thank you for editing!

To all of my friends who have suffered this experience with me, thank you for pushing me. Hugo, "Thank you for forcing me to do this".

Lastly, thank you to my son, Jaxon Christopher Elijah Roan. Thank you for your patience and love, and for believing in me. You are my motivation. I love you more than you know!

## DEDICATION

This work is dedicated to my family.

## TABLE OF CONTENTS

ABSTRACT.....	ii
ACKNOWLEDGEMENTS.....	iv
DEDICATION.....	v
LIST OF TABLES.....	viii
LIST OF FIGURES.....	ix
CHAPTER I.....	1
Background.....	1
Introduction.....	1
The insulin molecule.....	3
The insulin receptor.....	4
The insulin signaling pathway.....	6
Insulin receptors localize to microdomains.....	8
Cell membrane composition.....	10
Lipid packing.....	12
Lipid raft sphingolipid synthesis and cycling.....	14
Effectors of insulin signaling and lipid raft components.....	16
Free fatty acids in insulin signaling and lipid metabolism.....	18
Oxidative stress in insulin signaling and lipid metabolism.....	19
Lipid peroxidation in insulin signaling and lipid metabolism.....	20
Vanadium and other transition metal compounds with insulin enhancing activity as novel therapies.....	21

Vanadium and phosphorylation.....	22
Vanadium and reactive oxygen and nitrogen species.....	22
Vanadium and the plasma membrane.....	23
Anisotropy as a method of membrane fluidity measurement.....	24
TMA-DPH membrane probe.....	28
 CHAPTER II	
Evaluating membrane fluidity using Time-Correlated Single Photon Counting	
Fluorescence Anisotropy.....	30
Introduction.....	30
Materials.....	30
Methods.....	31
Cell culture.....	31
Cell counting protocol.....	32
Instrument parameters for anisotropy measurements .....	32
Treatments.....	33
Results.....	35
Discussion.....	39
CONCLUSIONS AND FUTURE DIRECTIONS.....	42
REFERENCES.....	45
LIST OF ABBREVIATIONS.....	51

## LIST OF TABLES

Table 1	Experimental design.....	34
---------	--------------------------	----

## LIST OF FIGURES

Figure 1	Molecular structure of insulin.....	4
Figure 2	Insulin receptor structure.....	5
Figure 3	Insulin signaling pathway.....	8
Figure 4	Insulin receptors in rafts/microdomains.....	9
Figure 5	Eukaryotic cell plasma membrane model.....	11
Figure 6	Lipid packing and distribution effects on order.....	13
Figure 7	Sphingolipid synthesis and degradation cycle.....	15
Figure 8	Inflammation and lipid peroxidation.....	17
Figure 9	Chemical structure of BMOV and BEOV.....	24
Figure 10	Z-axis orientation of a fluorophore.....	26
Figure 11	Schematic of instrumentation for time-correlated single photon counting anisotropy measurements.....	28
Figure 12	Chemical structure of membrane fluorescent probe TMA-DPH.....	29
Figure 13	Effects of a 390nm short pass filter on TCSPC anisotropy measurements.....	36
Figure 14	Experiment 1.....	37
Figure 15	Experiment 2.....	38
Figure 16	Experiment 3.....	39

## CHAPTER I

### BACKGROUND

#### INTRODUCTION

Diabetes mellitus is the leading cause of blindness, amputations, and cardiovascular-linked death with a post-diagnosis life expectancy worse than some forms of cancer (1). It is a debilitating metabolic disorder characterized by lack of insulin secretion or lack of response to insulin resulting in impaired metabolism of carbohydrates, lipids, and proteins. Type 1 diabetes results from the failure of the  $\beta$ -cells of the pancreas to produce insulin and accounts for 5-10% of diabetes cases. Type 2 diabetes, is characterized by insulin resistance, obesity, and dyslipidemia, and accounts for 90% of diabetes cases.

Obesity is one of the most common nutritional disorders in the United States whose prevalence has increased more than 75% since 1980 (2). Defined as a body-mass index in the 95<sup>th</sup> percentile or higher for age and sex, obesity is commonly recognized as increased lipid accumulation, as a result of nutrient oversupply, and is predicted to lead to a decline in life expectancy (3). Studies of obesity have been extensive due to the deleterious effects of excess lipids in the body (4). Obesity is known to lead to dyslipidemia, insulin resistance, eventually leading to the development of Type II Diabetes, and is associated with Metabolic Syndrome. (5-7).

While each of the above conditions can exist alone, they are traditionally found associated with one another and, due to the metabolic pathways involved, can potentiate the effects of one another (8). Insulin resistance due to obesity is usually a precursor to the development of Type II diabetes, which is estimated to exist up to 10 years prior to a formal diagnosis (9). Obese patients are typically found to be hyperglycemic and hyperinsulinemic.

The hyperinsulinemia is a result of being in a state of insulin resistance. The target tissues in the body are no longer responsive to the insulin being produced so the body responds by increasing the amount of insulin produced by the  $\beta$  cells of the pancreas. The hyperglycemia exists because the tissues are not able to respond to the insulin secreted and therefore have impaired uptake of glucose by the target cells. It has been noted that some individuals have a decreased affinity of the insulin receptor (IR) for insulin while others have normal binding of insulin but decreased intracellular response with decreased recruitment of the GLUT4 transporter to the cell surface in order to transport glucose into the cell (5-7).

Along with insulin resistance, obesity is known to produce dyslipidemia, a disruption in the amount of lipids in the blood and/or the ratios of lipids found in the blood when compared to a healthy individual. Excess lipids have been shown to accumulate in specialized tissues such as muscle, liver and heart (1). This has been noted in Metabolic Syndrome and Type II diabetes with the hallmark of high levels of triglycerides (TGs), increased low density lipoproteins (LDL) cholesterol and decreased high density lipoprotein (HDL) cholesterol levels (10).

Metabolic Syndrome is a cluster of metabolic derangements that include insulin resistance, obesity, hypertension, and dyslipidemia (9). While Metabolic Syndrome has received a great deal of attention, there is a lack of consensus as to whether metabolic syndrome actually constitutes its own diagnosis or is simply the sum of its parts (11,12). The treatment of metabolic syndrome is to treat each of its parts individually, the hypertension with hypertension medications, the insulin resistance with hyperglycemic medications, the dyslipidemia with drugs targeting the lowering of TG and LDL and the elevation of HDL's in the blood stream, hoping to prevent or slow the development of Type II diabetes in the patient (13-15). In order to

understand the relationships between excess lipids and the many signaling pathways involved in metabolic derangements, we will first look at insulin and the insulin signaling pathway.

## THE INSULIN MOLECULE

Insulin and the insulin-signaling pathway have been extensively studied due to their involvement in disease progression and glucose homeostasis. Insulin is the most potent anabolic hormone and is involved in synthesis and storage of carbohydrates, lipids and proteins as well as inhibiting degradation and subsequent release into circulation (16). Specifically, insulin is produced in the Islets of Langerhans in the pancreas by the  $\beta$ -cells and is composed of 51 amino acids. The action of insulin is mediated by the insulin receptor.

## THE INSULIN RECEPTOR

The insulin receptor (IR) is a tyrosine kinase transmembrane protein. It consists of two  $\alpha$ - and two  $\beta$ -subunits bound by disulfide bonds. Upon insulin binding to the  $\alpha$ - subunit on the extracellular surface of the cell, a conformational change occurs which results in ATP binding the  $\beta$ -subunit's intracellular domain (18). The  $\beta$ -subunit has extracellular, transmembrane and cytosolic regions. Upon ATP binding, autophosphorylation occurs on the cytosolic domain on three clusters of tyrosine residues (19). Once phosphorylated, the IR catalyzes the phosphorylation of several intracellular targets such as, insulin receptor substrate protein 1 (IRS-1), Shc, APS, and c-Cbl.

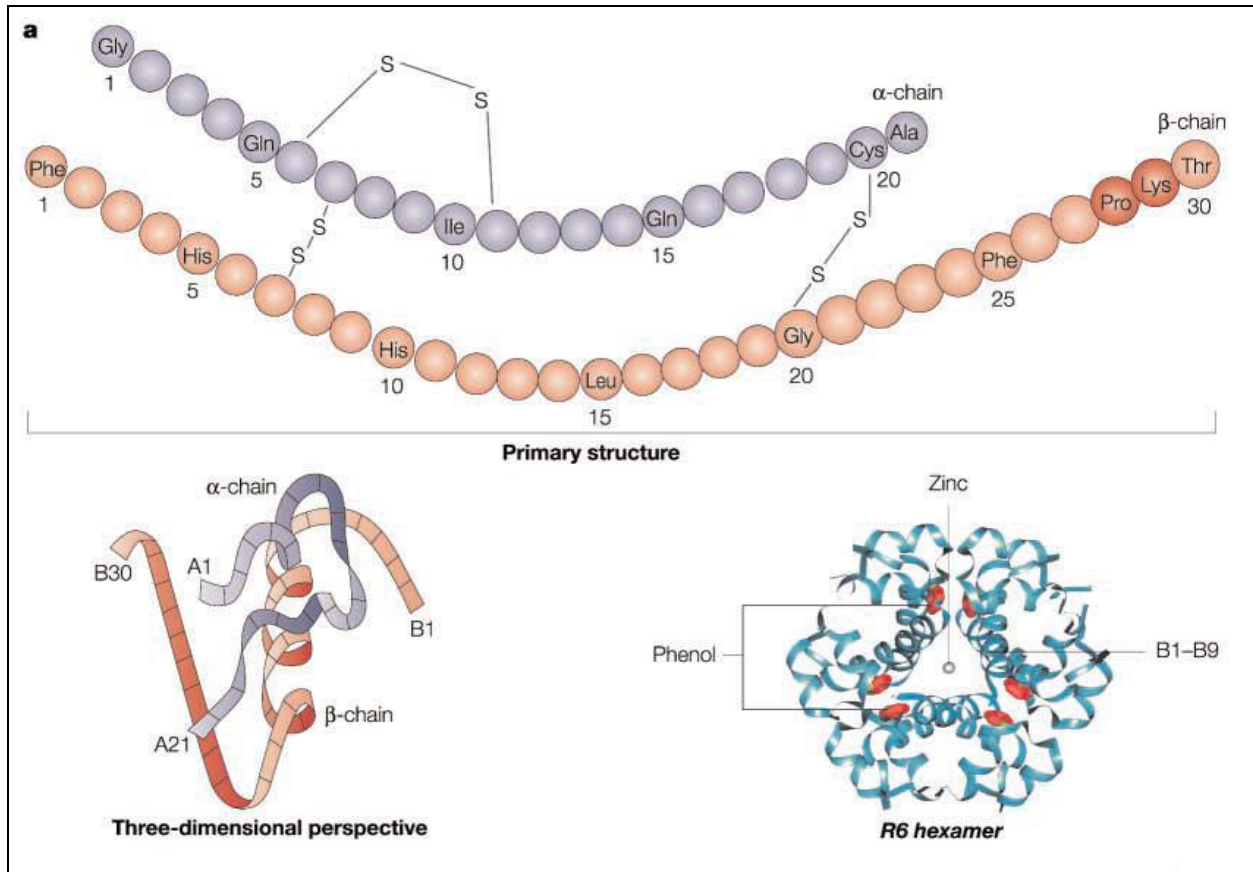


Figure 1. Molecular structure of insulin. Shown here in its primary structure showing the alpha and beta chains with disulfide bridges, a three dimensional representation and as a hexamer (17). (Adapted from Owens, D., Nature Reviews, 2002, 1:529-540.)

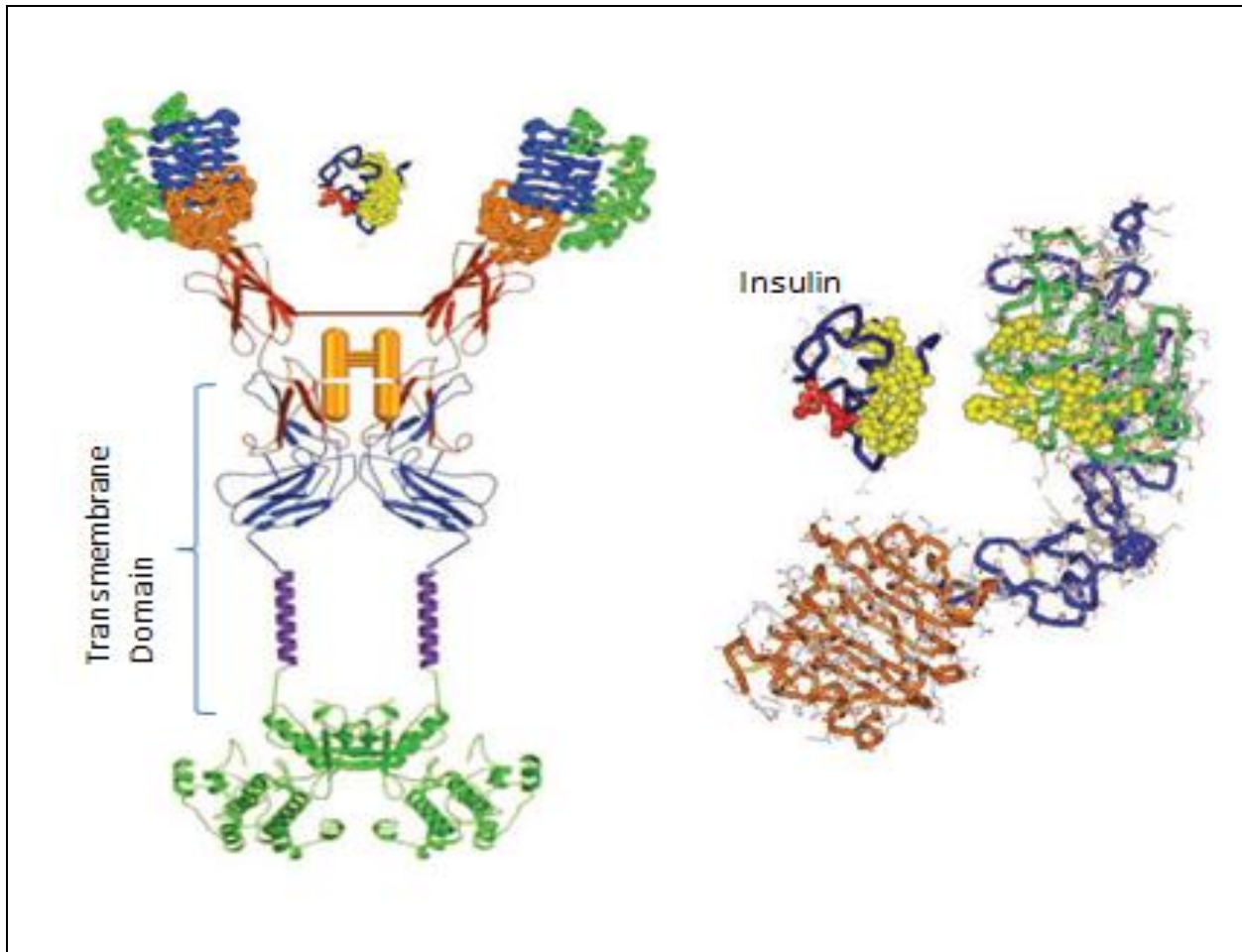


Figure 2. Computer generated 3-D modeling of the insulin receptor structure. Also shown is the relative size of the insulin molecule and its orientation in the receptor when binding. The insulin receptor has an extracellular domain which binds insulin, a transmembrane domain (labeled) which crosses the cell's plasma membrane, and a cytoplasmic domain (represented in green) which contains the portion of the receptor that undergoes autophosphorylation upon binding of insulin (20). (Adapted from De Meyts, P., and Whittaker, J. *Nature Reviews*, 2002, 1: 769-783.)

## THE INSULIN SIGNALING PATHWAY

When considering the insulin signaling pathway shown in Figure 3, attention must be paid to each site of phosphorylation. Sites of phosphorylation may serve as points of potential regulation. Signaling proteins with Src homology (SH2) domains are recruited by those targets and interact with the sequences surrounding the phosphotyrosines. Specific to IRS-1 family members is the generation of a docking site for p85, a regulatory subunit of type 1A phosphatidylinositol 3-kinase (PI3K) (18,21). PI3K phosphorylates phosphatidylinositol-4,5P2 (PIP2) to generate phosphatidylinositol-3,4,5-triphosphate (PIP3). PIP3 acts as the allosteric regulator of phosphoinositide-dependent kinase (PDK1), which phosphorylates and activates Akt and atypical protein kinase C isoforms PKC $\zeta$  and PKC $\lambda$  (22). PKC's are responsible for generating glucose uptake via the GLUT-4 transporters in muscle cells and adipocytes. While Akt and PI3K are known to play a role in GLUT4 translocation, there exists a PI3K independent pathway for GLUT4 recruitment. Cbl phosphorylation via insulin, associates with the CAP adaptor protein. This causes the Cbl-CAP complex to translocate to lipid rafts, or microdomains (MDs) in the plasma membrane. These will be discussed later in detail. At the MD, Cbl interacts with Crk, an adaptor protein, which is constitutively associated with the Rho-family guanine nucleotide exchange factor C3G. C3G activates TC10, a member of the GTP-binding protein family, which promotes GLUT4 translocation to the plasma membrane (23). Akt can activate 1) glycogen synthesis through glycogen synthase kinase 3 (GSK3), 2) gene expression through FKHR, and 3) protein synthesis by p70S6K (18). GSK3 acts on glycogen synthase, an enzyme that catalyzes the last step in glycogen synthesis. Once GSK3 phosphorylates glycogen synthase, it has effectively inhibited glycogen synthesis. Therefore, Akt inactivation of GSK3 promotes glucose storage as glycogen. Through phosphorylation and dephosphorylation events,

insulin blocks gluconeogenesis and glycogenolysis by the liver by controlling the expression of certain genes that encode for specific proteins required for gluconeogenesis (23). Synthesis of lipids is also controlled by insulin, as well as their degradation. This occurs through the transcription factor steroid regulatory binding protein SREBP-1. In adipocytes, glucose is stored as lipid and insulin inhibits lipolysis by blocking lipase, an enzyme sensitive to the hormone (23). Having discussed the cellular targets interactions and functions for insulin binding the IR, the insulin receptor can bind more than just insulin.

One of the unique features of the insulin receptor is its ability to bind insulin-like growth factor (IGF-1 and IGF-2). The affinity for binding these ligands is 100-1000 times lower than the receptor's affinity for insulin, but the circulating concentration of IGF-1 is around 100 times higher. IGF-2 has equal affinity for IRs and its own receptor. IGF-1 and IGF-2 also act by phosphorylating tyrosine residues on the IRS family of molecule (18). Binding of insulin-like growth factors leads to a growth response in the cell. The ability of the IR to bind more than one ligand may also be a point of regulation with attention to be paid to the possible changes in concentration of ligands in response to the stresses associated with metabolic syndrome. The termination of signals from the IR has been linked to events following ligand dissociation.

Once insulin dissociates from the receptor, its substrates undergo rapid dephosphorylation, which implicates protein tyrosine phosphatases (PTPases) in signal termination. Lipid dephosphorylases can also exert temporal control by dephosphorylating PIP3. Vollenweider *et al.* demonstrated that microinjection of phosphoinositide phosphatase SHIP2, blocks insulin action (24). Another area of investigation for IR function has been distribution and localization.

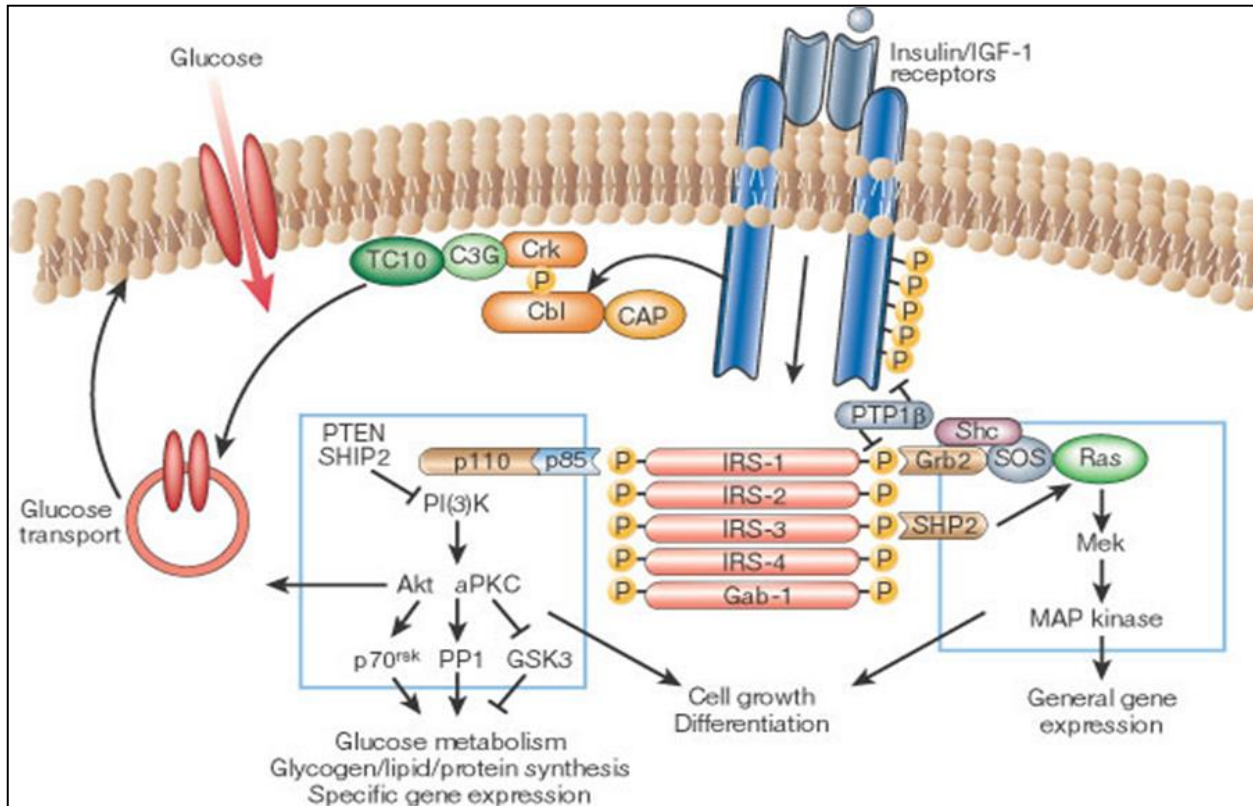


Figure 3. The insulin signaling pathway. Pathway activation can have multiple effects including glucose uptake, glucose metabolism, synthesis of glycogen, fats and proteins, and gene expression. Depending on the pathway activated, the response to binding ligand can be varied (23). (Adapted from Saltiel, A. R.; Kahn, C. R. *Nature*, 2001, 414: 799-806).

### INSULIN RECEPTORS LOCALIZE TO MICRODOMAINS

Key to optimal IR function, is its localization to small membrane regions known as lipid rafts, a specialized subset of microdomains (MD) that are enriched in sphingomyelin and cholesterol (23,25-27). Upon binding insulin, the IR's move into the MDs which serve as platforms on the exoplasmic leaf of the lipid bilayer (28). One of the characteristics of MDs is their ability to include or exclude certain proteins selectively, with the affinity for a particular protein being influenced by both intra- and extracellular stimuli. Interactions between adaptors

and scaffold and anchoring proteins can be organized through microdomains to transduce the signal leading to amplification through signal molecule concentration and the exclusion of unwanted modulators (29). Interestingly, MDs and their interactions with IRs in the insulin-signaling pathway can vary according to the tissue type involved. In adipocytes, IRs associate with a subset of MDs known as caveolae as seen in Figure 4 (29,30).

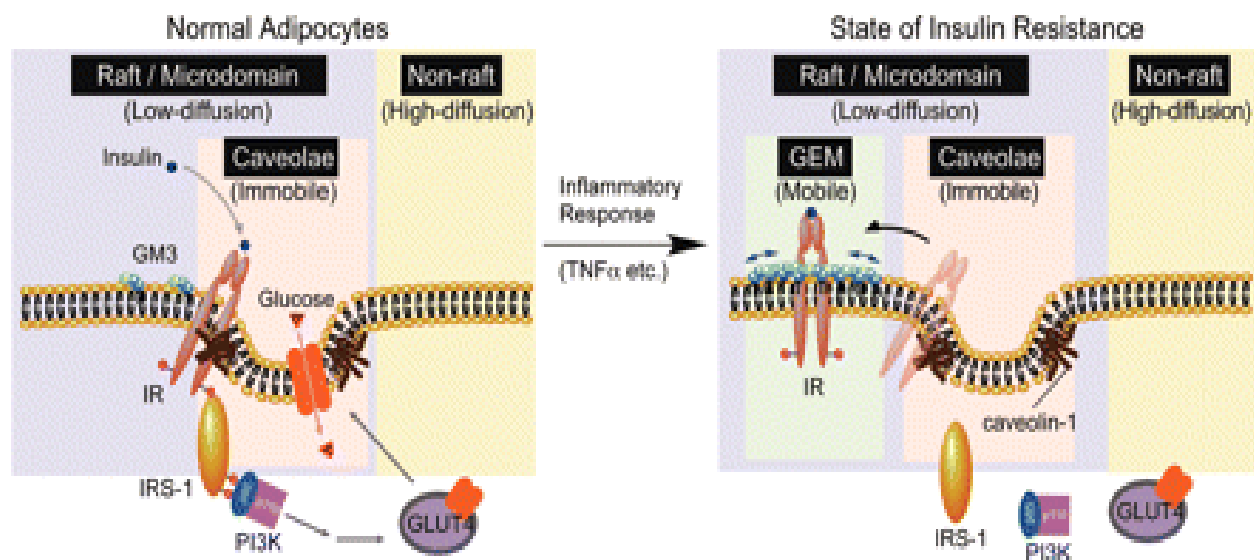


Figure 4. Insulin receptors associated with caveolin-enriched caveolae, a subset of microdomains. Caveolae may or may not be required for all insulin signaling, depending upon the tissue of interest, but a general microdomain enriched in cholesterol and sphingomyelin is required. The relationship between IR distribution and insulin resistance in response to inflammation is also shown (31). (Adapted from Kabayama *et al. Glycobiology* 2005, 15: 21-29.)

Caveolae are small, flask shaped, non-clatharin-coated invaginations in the plasma membrane (PM) that are rich in the protein caveolin (32,33). Caveolin also associates with the GLUT4 glucose transporter in adipocytes (33). Though found intracellularly, caveolin in the PM exists only in caveolae, whose proper function depends on a sufficient level of cholesterol (34). However, in the liver, the IR does not require calveolae within the MD, in order to function

properly, though it is still associated with a lipid raft region in the plasma membrane that is enriched with cholesterol (28). The variability of the localization of the IR, based on tissue distribution, implies that the features that regulate responses through IRs in MDs are specialized. In order to understand the specialized role that MDs play in signaling, we must understand the distribution of lipids within the PM.

## CELL MEMBRANE COMPOSITION

The plasma membrane has been a subject of study for many years. Basic science textbooks include descriptions of the fluid mosaic model of the membrane first proposed by Singer and Nicolson in 1972 which described a bilayer of lipids with different proteins scattered throughout (35). Since then, research has revealed that the PM is more complex and dynamic than initially believed. Heterogeneity exists between the extracellular side of the PM and the cytosolic side. The distribution of phospholipids on the extracellular leaflet has a large concentration of phosphatidylcholine (PC) and sphingomyelin (SM). The cytosolic leaflet is preferentially composed of phosphatidylethanolamine (PE) and phosphatidylserine (PS) (36-39). A brief review of the production of the membrane lipids is given below.

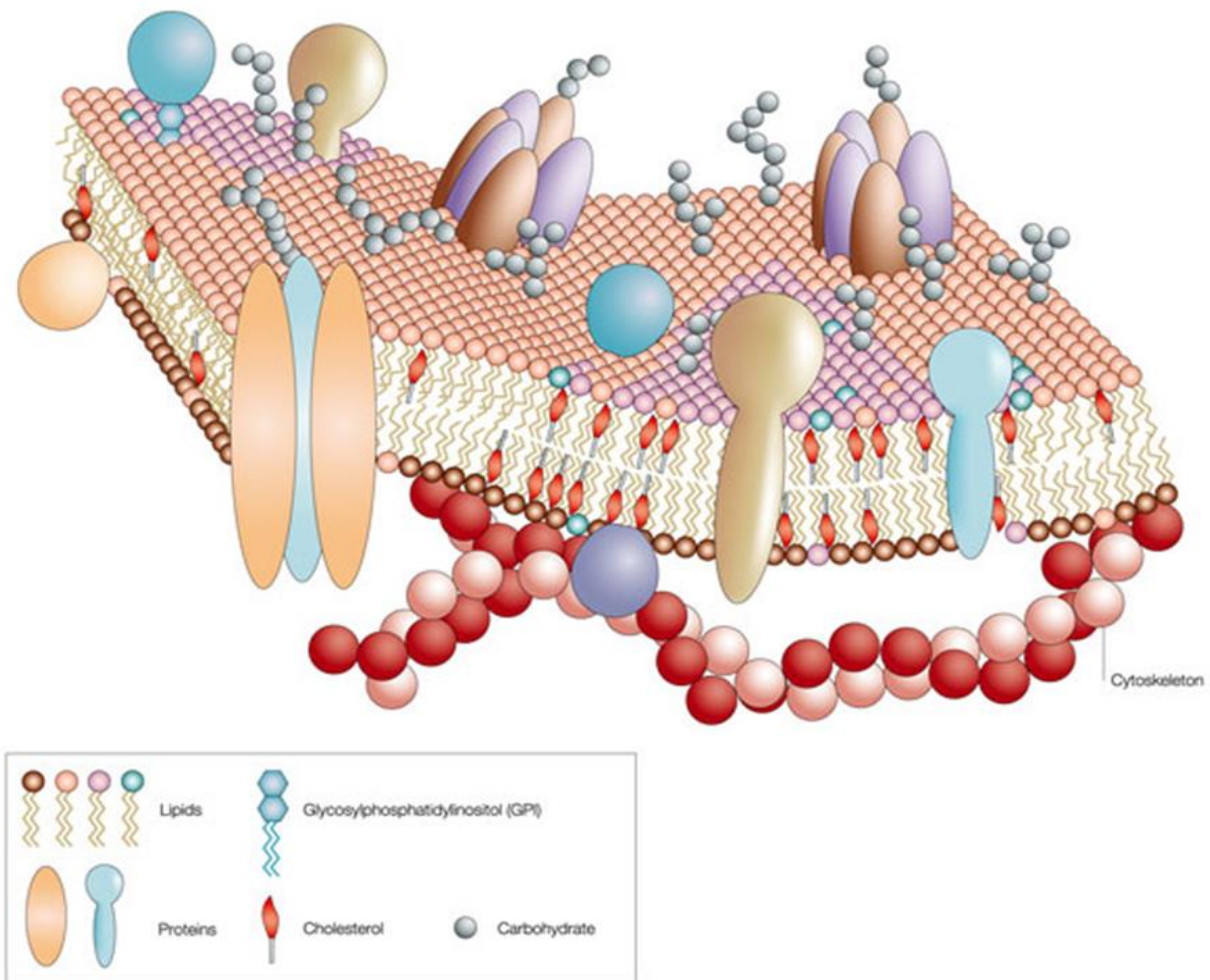


Figure 5. Model of a cell's plasma membrane demonstrating heterogeneity in the distribution and location of phospholipid constituents and cholesterol. Various types of membrane associated proteins are also modeled as well as the associated cytoskeleton on the cytoplasmic side of the plasma membrane bilayer (40). (Adapted from Pietzsch, J., *Nature*, 2004, Horizon Symposia: Living Frontier, 1-4.)

The lipid elements of the membrane are initially constructed in the smooth endoplasmic reticulum (SER), specifically the glycerophospholipids which are synthesized on the cytoplasmic side of the SER. From the SER, the phospholipids are transferred to the Golgi. Within the Golgi it has been found that the asymmetry of the membrane bilayer is established. Specific proteins in

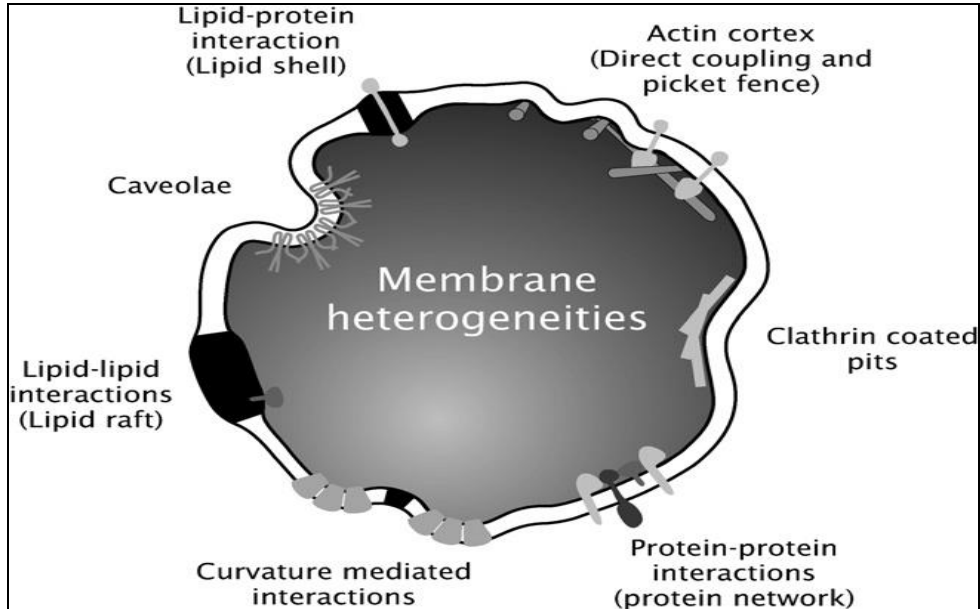
red blood cells, termed flippases, floppases, and scramblases, have been found to be responsible for redistributing and orienting the phospholipids for vesicular transport to the PM so that they are appropriately matched for fusion with the PM bilayer (36,37). Flippases are responsible for “flipping” lipids toward the cytoplasmic side of the membrane and floppases move lipids in the opposite direction. Scramblases possess the ability to move lipids in either direction and have been found to be involved in apoptosis and cell signaling (41). In other types of eukaryotic cells, similarly functioning proteins have been identified (38, 42-44).

## LIPID PACKING

Within the PM exist specialized regions known as lipid rafts, previously mentioned in the section on the insulin signaling pathway. These subsets of MDs are unique in their composition of high concentrations of sphingomyelin (SM) and cholesterol. It has been found that cholesterol may play a role in phase separations as it prefers to associate with saturated lipids. When a lipid is saturated, it lacks conformational changes in its fatty acids resulting in the ability to package themselves more closely together. This packing is described as being “liquid-ordered” (LO). The surrounding membrane is considered “liquid-disordered” (LD) as it has a larger concentration of unsaturated lipids and thus cannot spatially organize into a tighter conformation as seen in Figure 6 (45-48).

Given the specificity of the distribution of phospholipids to their respective sides of the PM bilayer and the specialized function and composition of lipid rafts and lipid packing in MD formation, it is important to next examine the effects that obesity and insulin resistance may have on the membrane components involved in insulin signaling.

a).



b).

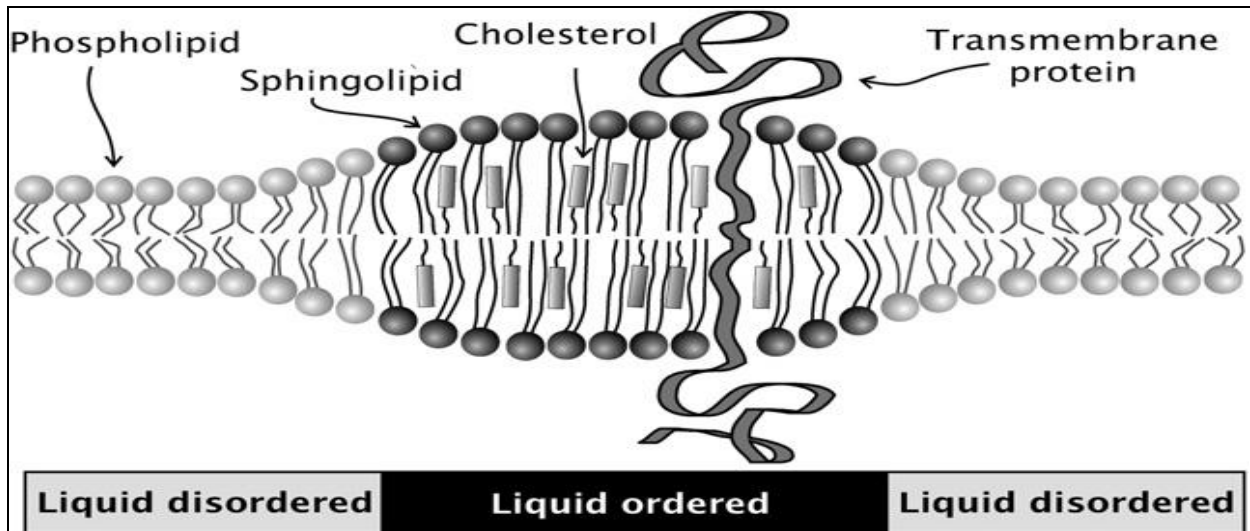


Figure 6. a). Model of lipid interactions with components distributed in the cell membrane including lipid rafts, caveolae, clathrin coated pits and the cytoskeleton. b). Representation of lipid packing in lipid rafts and the effects on the level of order in the membrane (49). (Adapted from (Semrau, S., and Schmidt, T., *Soft Matter*, *J. Royal. Soc. Chem.* 2009, 5: 3174-3186.)

## LIPID RAFT SPHINGOLIPID SYNTHESIS AND CYCLING

Sphingolipids consist of sphingophospholipids and sphingoglycolipids, and are major players in MDs in the plasma membrane even though they only make up a small portion of lipids found in the plasma membrane. As seen in Figure 7, the major component of sphingolipids is sphingomyelin (SM) which contains a head group that is either phosphocholine or phosphoethanolamine (50). The structure of SM includes a long-chain saturated or monounsaturated fatty acid, a head group, and a sphingosine base backbone. In the smooth endoplasmic reticulum (SER), *de novo* synthesis of SM occurs. Ceramide formation begins with the synthesis of sphinganine followed by the transfer of an acyl group, this forms acylsphinganine (dihydroceramide). This product is oxidized to form ceramide. Then the phosphocholine head group is attached by SM synthase. SM can be turned over by removal of the head group by sphingomyelinases (SMases) and the removal of amide-linked fatty acid by ceramidases. While *de novo* synthesis of ceramide has already been mentioned, of interest is its involvement in the SM pathway, which involves the hydrolysis of SM to form ceramide. Ceramide levels have been shown to be elevated in numerous rodent and human models with insulin-resistance (51). Ceramide has also been shown to be pro-apoptotic as *de novo* Fas activated pathway activates PP1, a ceramide-activated Ser-Thr phosphatase. PP1 then dephosphorylates proteins that regulate RNA splicing which results in a pro-apoptotic mRNAs being favorably translated (52). Thus *de novo* synthesis, as well as SM hydrolysis, is important because SM is an integral component of MDs and a potential target for IR loss of function (50).

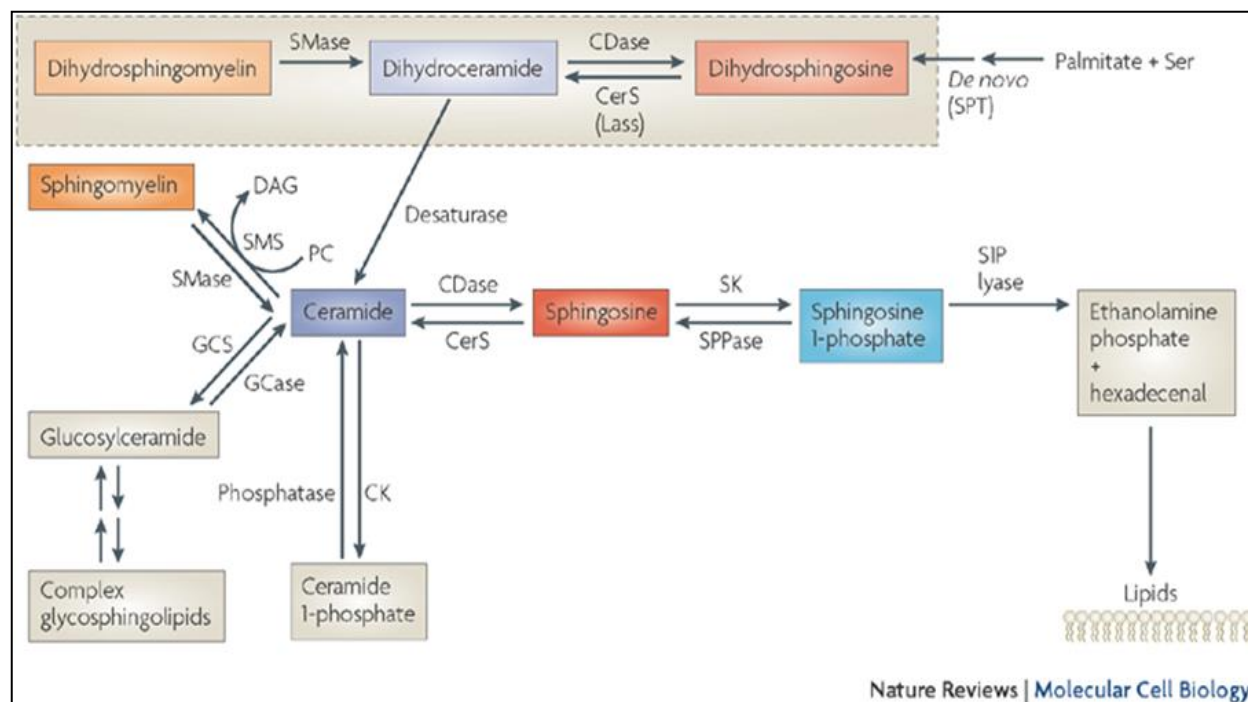


Figure 7. Sphingolipid synthesis and degradation cycle. Ceramide has been identified as a key player in the production and degradation of sphingomyelin and is shown in dark blue. This may serve a marker for lipid cycling or peroxidation (52). (Adapted from Hannun *et al.* *Molecular Cell Biology* 2008, 9: 139-150).

In the SM pathway, SMases, as mentioned, are responsible for the removal of the phosphocholine head group on SM. SMases exist as acidic, neutral, or alkaline SMases and are localized based on their optimal pH. Acidic SMases exist in lysosomes whereas neutral and alkaline SMases are located in or near the PM. Ceramide, itself, can inhibit SMase activity. SM synthase catalyzes the reverse reaction of SMases by increasing the rate at which phosphorylcholine is transferred from PC to ceramide to yield diacylglycerol (DAG) and SM (50). Ceramide can vary in chain length and can be broken down into sphingosine and a free fatty acid (FFA) via ceramidase (CDase). Sphingosines produced by CDases can be phosphorylated by sphingosine kinase to produce sphingosine 1-phosphate (S1P). S1P has been

shown to oppose the action of ceramide (53). However, this pathway can be manipulated by an excess of lipid.

## EFFECTORS OF INSULIN SIGNALING AND LIPID RAFT COMPONENTS

Metabolic derangements, triggered by high-calorie diets and a lack of exercise, are associated with increased adipocyte proliferation and inflammation. Inflammation can affect cell signaling pathways through a number of mechanisms. Mechanisms include production of inflammatory cytokines and increasing oxidative stress resulting in an imbalance in regulation of the cell's redox chemistry. This imbalance results in production of reactive oxygen species (ROS) (54). ROS generation leads to increases in free fatty acids (FFAs) by interacting with the cell membrane and oxidizing lipid components which is known as lipid peroxidation. How these mechanisms overlap both the insulin signaling pathway and lipid metabolism is of great interest in trying to elucidate the mechanisms of action of potential drugs and for targeting drug therapy.

Excess lipids have been linked to inflammation resulting in the activation of inflammatory cytokines (56). One such cytokine that has received a lot of attention is TNF- $\alpha$  (Figure 8). TNF- $\alpha$  is produced at greater levels by the excess adipose tissue in obese individuals as well as the protein resistin which together both act to impair IR function. TNF- $\alpha$  can activate serine threonine kinases like JNK and IKK $\beta$ , already previously mentioned as IRS inhibitors in the insulin signaling pathway. TNF- $\alpha$  can not only inhibit IRS function, it has been shown to affect the transcription of cytokine signaling-3, a protein that interacts with the IR and IRS protein.

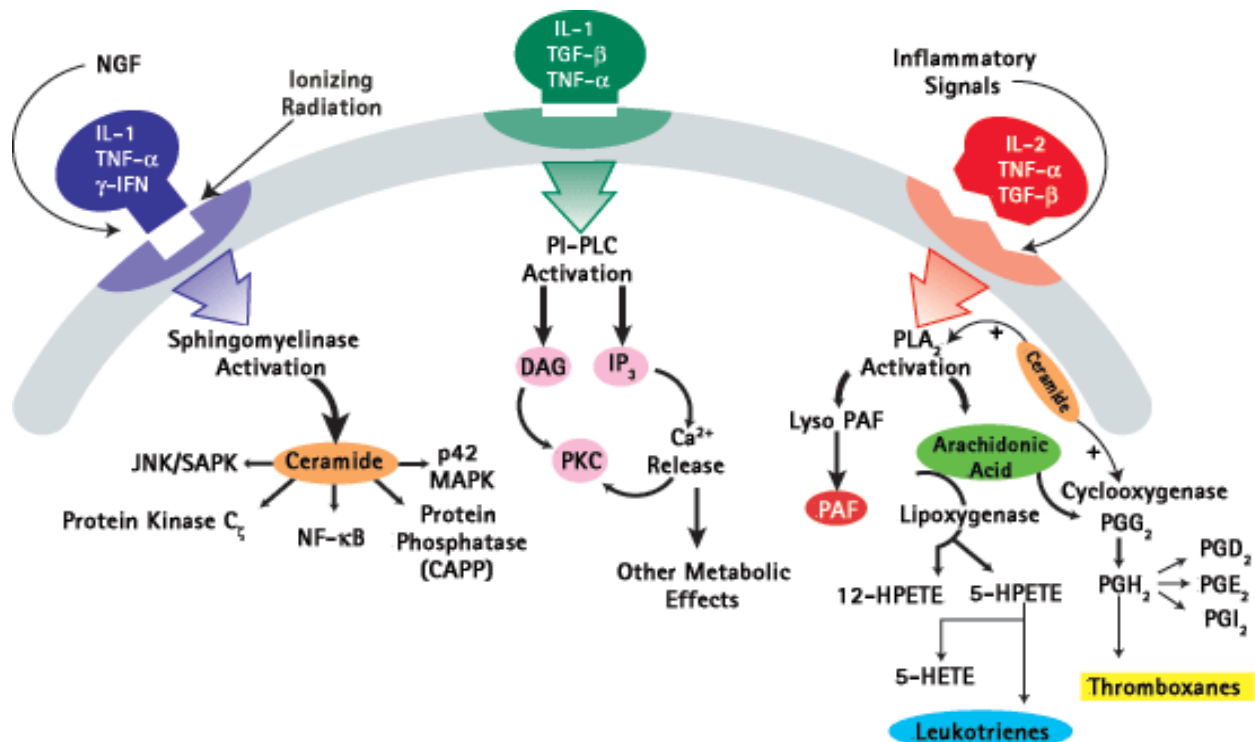


Figure 8. Inflammation and lipid peroxidation. Multiple pathways are involved in lipid peroxidation and degradation in response to inflammatory cytokines or ionizing radiation. Of note is the formation of ceramide which is implicated in multiple pathways including the arachidonic acid pathway which produces leukotrienes and thromboxanes, both of which contribute to the pro-inflammatory and pro-thrombotic states found in insulin dysregulation (55). (Adapted from the Merck Biosciences website, [www.merckbiosciences.co.uk](http://www.merckbiosciences.co.uk)).

However, these are not the only ways in which TNF- $\alpha$  can act. A study by Kabayama *et al*, showed that TNF- $\alpha$  induces an overproduction of GM-3 ganglioside (57). This overproduction leads to an insulin-resistant state by GM-3s displacement of the IR from the MDs (57). This suggests that there may be some preferential interaction with the lipids of the MD that GM-3 may possess over the IR. Another way in which TNF- $\alpha$  affects MDs is that it alters the rates of lipid hydrolysis by rapidly increasing the amount of ceramide produced by breaking down SM as well as promoting *de novo* synthesis of ceramide as well (58-60). The equilibrium

that exists in sphingolipid metabolism between formation of SM or hydrolysis to ceramide raises the question that if ceramide levels have been shown to be elevated in insulin-resistant models, and IR loss of function can be linked to its association, or lack thereof, with MDs, is the hydrolysis of SM to ceramide one cause of what has been seen? While ceramide has been implicated in effects on Akt(PKB) and subsequent inhibition of glucose uptake, a recent study found that ceramide can also block actin remodeling. The inhibition was found to be a result of a lack of activation of Rac which decreased GLUT4 translocation (61). Therefore, an inflammatory response by TNF- $\alpha$ , can increase ceramide production and result in attenuation of insulin signaling via combinatorial mechanisms. Increases in ceramide levels likely will result in increased enzymatic breakdown by CDases resulting in sphingosine and a FFA. Free fatty acids have also been implicated in a loss of insulin signaling and changes in regulation of lipid handling by the cell.

#### FREE FATTY ACIDS IN INSULIN SIGNALING AND LIPID METABOLISM

Free fatty acids have also been shown to have a role in insulin-resistance. Non-esterified fatty acids (NEFA) can affect insulin signaling via inhibition of PKB (Akt), thereby blocking glucose uptake. NEFAs can decrease the IRS-1 tyrosine phosphorylation by producing an inhibitory Ser<sup>307</sup> phosphorylation by PKC $\theta$  (62).

Adipocytes are capable of esterifying NEFAs into triglycerides and then sequester the triglycerides into lipid droplets (63). Within adipocytes, elevated FFA plasma levels are sensed by nuclear receptors known as peroxisome proliferator-activated receptors (PPARs). These control fatty acid degradation and storage, as well as adipocyte differentiation (54). Lipid chaperones in adipocytes called fatty acid binding proteins (FABPs) coordinate lipid metabolism

responses. Interestingly, animals lacking FABP4 and FABP5 exhibited similar fatty acid resistance found in human and mouse models similar to the effects of PPARs, as well as protection from most features of metabolic syndrome (64,65). This demonstrates that increased free fatty acids can affect lipid metabolism via PPARs and FABPs. Free fatty acids are produced as part of normal lipid metabolism as well as inflammation which can lead to increases in oxidative stress .

## OXIDATIVE STRESS IN INSULIN SIGNALING AND LIPID METABOLISM

Oxidative stress (OS) is defined as an oxidant/antioxidant system equilibrium imbalance where the oxidant side dominates, and as such, has been implicated in the degeneration of conditions associated with diabetes (66). OS has been shown to decrease pancreatic  $\beta$ -cell insulin secretion, as well as impair glucose uptake in muscle and fat as well as decrease pancreatic  $\beta$ -cell insulin secretion (67). Many studies have focused on oxidative stress in relation to Type II diabetes, and insulin-resistance, and have found increased levels of OS and ROS generated in both rodent and human experiments (68-70). Cardona *et al.* demonstrated that an increase in oxidative stress occurs in subjects with and without metabolic syndrome when given a high fat meal by increasing TG rich lipoprotein plasma levels. The increase in TGs levels lead to increases in free radicals from lipids and ROS (1). The authors did note that this was not the only source of oxidative stress, acknowledging the effects of hyperglycemia which results in increased inflammation. They also noted the potential of the mitochondria to produce ROSs. The mitochondria is a primary source of electron and oxygen handling in the cell and has also been identified as a source of proteins involved in lipid droplet formation and lipolysis regulation (71). While proteins associated with the mitochondria have some control in lipid

metabolism, ROSs can also affect lipolysis by interacting with the cell membrane leading to lipid peroxidation. Antioxidant enzymes have been demonstrated to be part of the regulation of ROS in the cell. ROSs levels elevate with a decrease in antioxidant enzyme concentrations (70).

Regulation of ROSs includes the antioxidant defense. The antioxidant defense was described as a network of enzymes including glutathione peroxidase (GPx), and antioxidants that are non-enzymatic. GPx is a seleno-enzyme, meaning it contains selenium which is required for its function. Some of the functions in which GPx is involved are signaling pathways of cell death and survival, protein kinase phosphorylation, and oxidant-mediated activation of NF $\kappa$ B as well as maintaining lipid peroxide levels (72). Interestingly, studies described in the review by Lei *et al.* showed that GPx-overexpressing mice developed hyperglycemia, hyperinsulinemia, and insulin resistance (72). This is counter-intuitive as functioning Gpx is part of the antioxidant defense. This implies that the redox chemistry within the cell is in a state of equilibrium in that without sufficient GPx, lipid peroxidation proliferates. How lipid peroxidation affects insulin signaling and the cell membrane will be explained next.

## LIPID PEROXIDATION IN INSULIN SIGNALING AND LIPID METABOLISM

Lipid peroxidation occurs when ROS interact with the lipid components of the cell membrane. Levels of lipid peroxides were found to be higher in Type 2 diabetics compared to controls and Type 1 diabetics in a study by Cymbaljevic *et al.* (10). This is likely due to increased inflammation, free fatty acids, and oxidative stress secondary to excess adipose tissue seen in Type II diabetics.

Lipid peroxidation byproducts have recently been implicated in changes in human insulin structure and function. Pillon *et al.* demonstrated that adductions occur at the histidine residues

on the human insulin molecule when exposed to highly volatile lipid peroxidation byproducts. They then demonstrated that the efficacy of GLUT4 translocation and subsequent glucose uptake was significantly reduced in multiple models including 3T3-L1 adipocytes, L6 muscle cells, and the hypoglycemic effects of the modified insulin in mouse models was also significantly decreased (73). In a study done by Navarro *et al.* hydroxyl radicals introduced carbonyl groups to the native insulin molecule as well as tyrosine residue formation. The changes in the insulin molecule also resulted in ineffective glucose uptake in rat models and adipocytes (74). These data add to the growing body of evidence that inflammation and lipids play a large and multi-factorial role in the development of insulin resistance and diabetes. Investigations into potential therapies should include exploration of effects on both insulin and its pathway as well as any effects the potential therapy may have on the membrane.

#### VANADIUM AND OTHER TRANSITION METAL COMPOUNDS WITH INSULIN ENHANCING ACTIVITY AS NOVEL THERAPIES

Vanadium was used historically in France as a treatment for diabetes (75). It is generally recognized that insulin responsiveness can be enhanced and elevated blood glucose and lipid levels can be normalized by administration of specific vanadium compounds (76-81). Other transition metal compounds including chromium and molybdenum have also demonstrated insulin-enhancing properties both individually or in combination with vanadium (82-86). Interestingly, some the vanadium compounds studied did not interact with the insulin receptor (IR) directly, but acted intracellularly (81,87-90).

## VANADIUM AND PHOSPHORYLATION

One of the mechanisms of actions of certain vanadium compounds is to inhibit dephosphorylation by protein tyrosine phosphatases (PTPases) which results in sustained phosphorylation of intracellular proteins which then results in a lack of termination of signal. The lack of termination in signaling results in perpetuation of signaling (91-98). This has been demonstrated in adipocytes in insulin signaling and is thought to act via PI3K (99). With BMOV treated adipocytes, it was found that in the presence of insulin there was increased phosphorylation of the tyrosine residues of the IR as well as increased phosphorylation of IRS-1 (100).

In answer to the question whether it is the vanadium compounds or the ligands that effect insulin signaling, several investigations found that certain classes of vanadium compounds are found to enhance the activity of insulin with the metal with a greater affect than the ligand alone. In recent studies, the effectiveness varies with the oxidation state of the metal (101,102) and the various ligands exert a “fine-tuning” effect (79,103) to enhance insulin responsiveness in part by decreasing the toxicity of the metal within the body. A study by Barrand *et al.* noted that malto and ethylmalto ligands provided some protection against the gastrointestinal irritation that vanadium compounds can cause (104).

## VANADIUM AND REACTIVE OXYGEN AND NITROGEN SPECIES

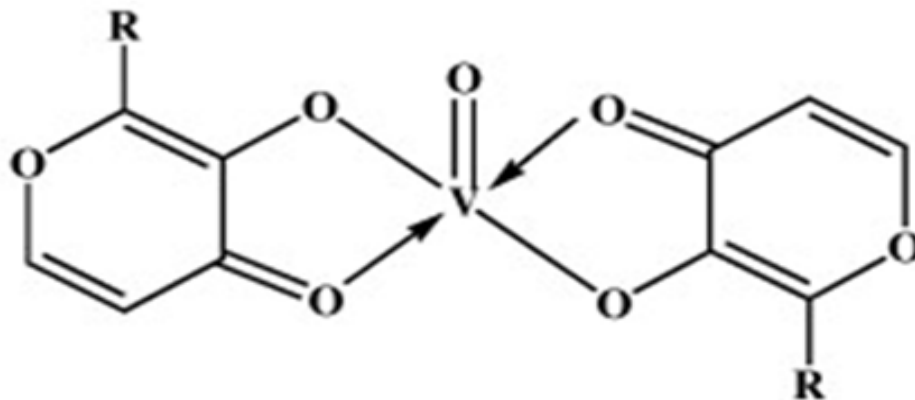
Vanadium compounds have been found to be involved with stress signaling pathways in the cell as well as apoptosis (87,105) have also been found to produce ROS and reactive nitrogen species (RNS) as well as affect glutathione levels in cells (106-109). As previously discussed, glutathione is involved in the antioxidant/oxidant balance in the cell and diabetes and obesity are

linked to increases in ROS generation. This apparent imbalance changes the redox state of the cell. Vanadium compounds are known to undergo redox cycling within the cell and this may be one mechanism of modulating the other players previously identified in the insulin signaling pathway.

## VANADIUM AND THE PLASMA MEMBRANE

While it has been demonstrated that some vanadium compounds exert their effects through PTP inhibition within the cell, it is worth examining the interactions of vanadium compounds with the PM. In order to gain access into the cell, vanadium compounds must interact with the cell's membrane. Recent findings demonstrate that the insulin-enhancing compound [VO<sub>2</sub>dipic] (110,111) penetrates the lipid interface and is located in the hydrophobic portion of the lipid layer of the microemulsion (112,113). Previous reports have shown the highly lipophilic vanadium compounds such as naglivan (114) are able to penetrate lipid monolayers (81,115). New evidence suggests that vanadium compounds can also affect membrane composition and lipid packing (116,117).

It is the seemingly multifactorial effect that vanadium compounds have on the insulin signaling pathway that warrants further investigation as to how these molecules exert their effects. In this study, BMOV was used as it is structurally similar to bis(ethylmaltolato)oxovanadium (IV) complex (BEOV) that has completed phase 1 clinical trials (118). See Figure 9 for a comparison of the two structures. What effects, if any, it has on the fluidity of the cell membrane may suggest a change in the lipid packing of the PM as a mechanism of action for affecting insulin receptor signaling.



R= CH<sub>3</sub>bis(maltolato)oxovanadium(IV), **BMOV**

R= C<sub>2</sub>H<sub>5</sub>bis(ethylmaltolato)oxovanadium(IV), **BEOV**

Figure 9. Molecular structure of BMOV and BEOV. Chemically and structurally, BMOV and BEOV are similar. BEOV began stage II clinical trials in 2008 and differs from BMOV by one additional hydro carbon (CH<sub>2</sub>). Abdol-Khalegh Bordbar *et al.* noted that much of the chemistry involved in the affinity of BMOV for binding human serum transferrin involved oxidation of the vanadyl (IV) ion (119). (Adapted from Abd-Khaegh Bordbar, A., *et al.*, *Journal of Inorganic Biochemistry* 2009.:103, 643–647.)

## ANISOTROPY AS A METHOD OF MEMBRANE FLUIDITY MEASUREMENT

Anisotropy uses polarized excitation of a sample and measures the intensity of the fluorescence emission through a polarizer. Polarized light preferentially excites fluorophores whose transition moments are aligned parallel to the excitation's polarization. The fluorescence from these molecules will also be parallel to the excitation. The mathematical equations for anisotropy have been derived by Lakowicz in his work, Principles of Fluorescence Spectroscopy (2006). Anisotropy is described mathematically as

$$r = \frac{I_{\parallel} - I_{\perp}}{I_{\parallel} + 2I_{\perp}} \quad (1)$$

A number of things can affect a measured anisotropy. For example, rotational diffusion of a fluorophore will affect measures of anisotropy by depolarization as the molecules transition moment changes. If the fluorescent molecule has freedom of motion prior to polarized excitation, the transition moment of the molecule will not be fixed and thus the probability of the molecule being oriented to the polarized excitation is low. Therefore the fluorophore is not likely to be excited. If the molecule is oriented to the polarized excitation and has freedom of motion following excitation, the angle at which the fluorophore will emit will not be parallel to the excitation polarization (120).

According to the author of Principles of Fluorescence Spectroscopy, the value for anisotropy,  $r = 1.0$ , if a single fluorophore is oriented along the z-axis as seen in Figure 10. However, the limit of  $r = 0.4$  is based on mathematical derivations from the probability distributions for molecules that will display maximal photoselection and is a function of  $\cos^2\theta$ . See Equation 2. The authors note that any value greater than  $r = 0.4$  is attributed to light scatter or multi-photon excitation.

$$r_0 = \frac{2}{5} \left( \frac{3 \cos^2\beta - 1}{2} \right) \quad (2)$$

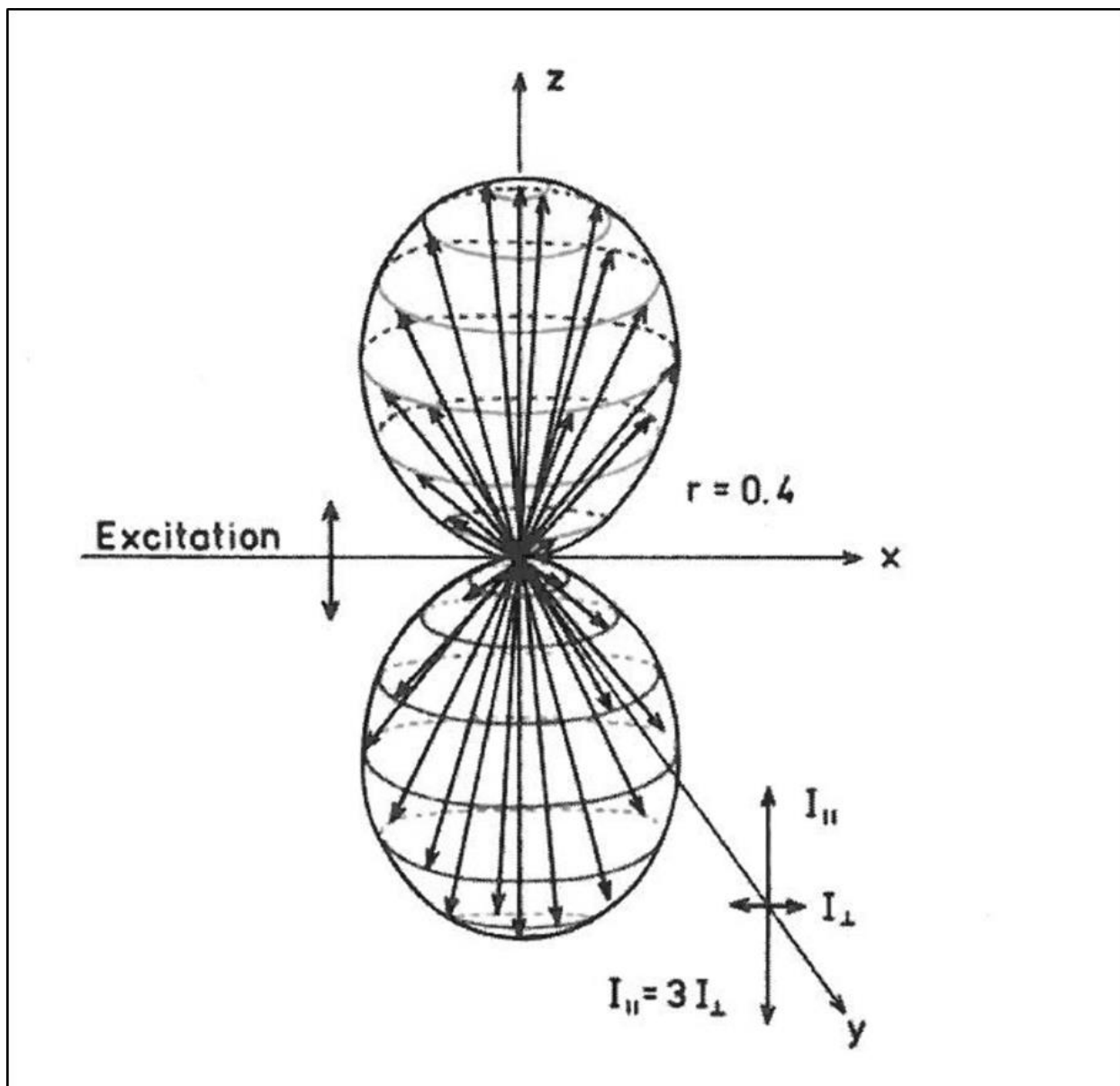
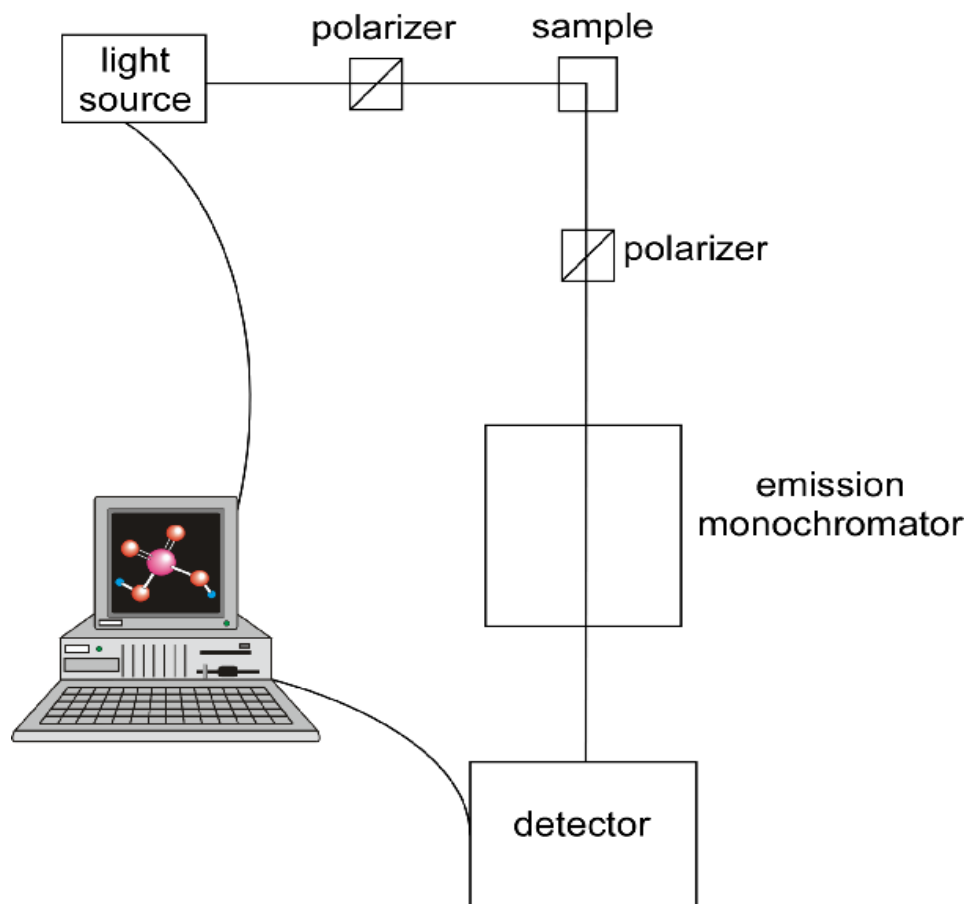


Figure 10. Z-axis orientation of the excited state distribution for an immobile fluorophore with an anisotropy of  $r = 0.4$  (120). (Adapted from Lakowicz, J. R. 2006. Principles of Fluorescence Spectroscopy. Springer, Berlin, Germany.)

When considering rotational diffusion, the viscosity of the environment plays an important role in how quickly a fluorophore can rotate or diffuse. When a fluorophore inserts itself into the PM, its position becomes fixed and is therefore capable of responding to polarized excitation. The fluidity of the PM can change in the face of changes in the environment of the

cell. When the PM becomes more fluid, the fluorophore is no longer in a fixed position and thus, there is a change in anisotropy. It is the resultant change in anisotropy that describes changes in the probe environment. For our experiments, we chose to use Time Correlated Single Photon Counting (TCSPC) Anisotropy. This method differs from steady state fluorescence anisotropy in that fluorescent decays model the photons of light being emitted over a period of time following the excitation from a source of light. Rather than measure every photon emitted for each excitation, TCSPC Anisotropy is a method used to detect one and only one photon emitted after fluorescence per pulse of light, for many, many pulses of light and is an averaging technique (120). Figure 11 is a detailed schematic of the instrument. The rationale for this method is that a fluorescent probe, when inserted in a lipid bilayer, will not display the typical decay to zero used in steady state anisotropy. It is this principle that demonstrates the restricted motion of the probe within a membrane and thus any changes in a timed anisotropy decay will yield information on how a treatment has affected the probe's environment (120). The equation used in evaluating time-dependent decays is

$$r(t) = \frac{I_{\parallel}(t) - I_{\perp}(t)}{I_{\parallel}(t) + 2I_{\perp}(t)} \quad (3)$$



## TCSPC experiment

Figure 11. Detailed schematic of the Time-correlated Single Photon Counting apparatus of the Jovin IBH used in the experiments (121). Image is courtesy of Laura Swafford of the Levinger lab at Colorado State University.

### TMA-DPH MEMBRANE PROBE

The fluorophore chosen for the fluidity measurements is the dye 1-(4-trimethylammoniumphenyl)-6-phenyl-1,3,5-hexatriene *p*-toluenesulfonate, (TMA-DPH) from Molecular Probes of Invitrogen. TMA-DPH is well characterized and has been used extensively to explore lipid membrane dynamics and characterization (122-124). TMA-DPH has a

maximum absorbance at 356nm and emits at 435nm. The carbon chain inserts itself into the outer leaflet of the membrane and the trimethylammonium component interacts with the polarized environment on the external surface of the cell.

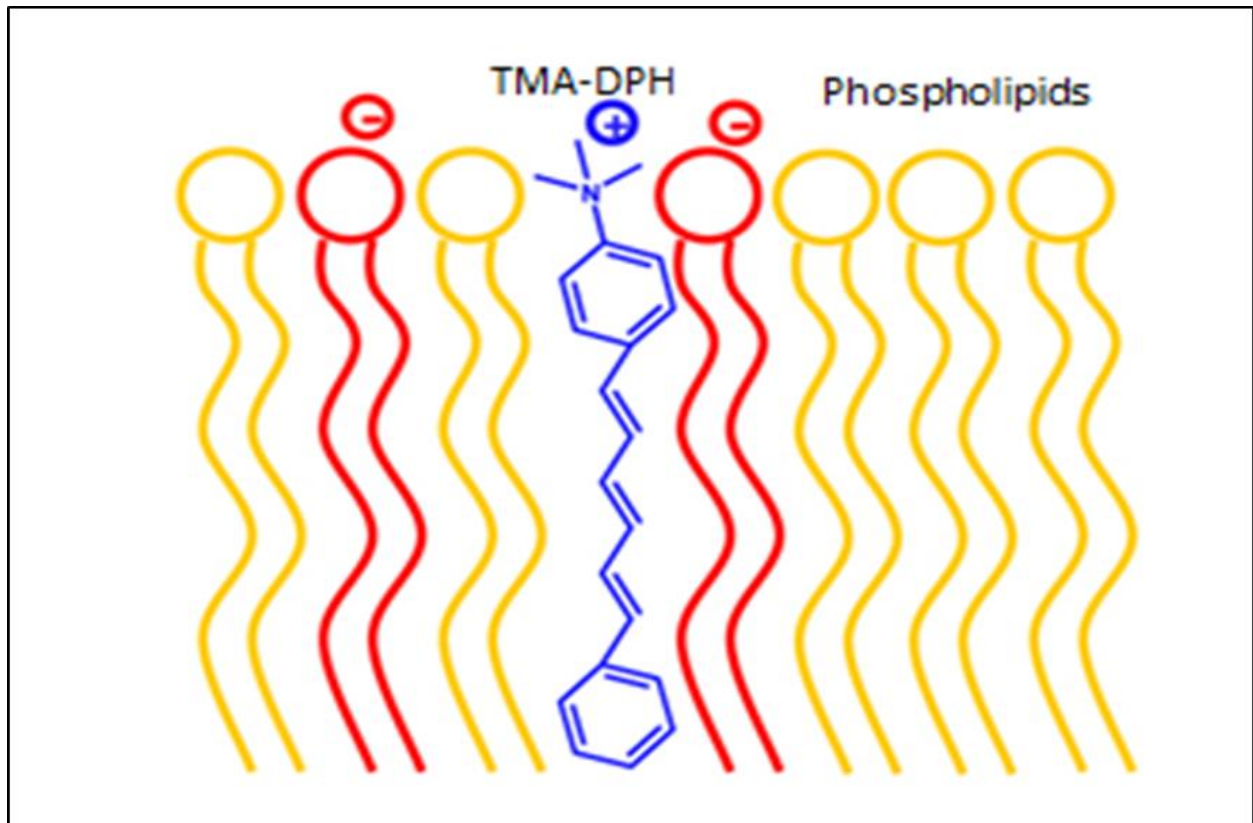


Figure 12. Chemical structure of membrane fluorescent probe TMA-DPH. TMA-DPH: is a suitable fluorescence polarization probe for specific plasma membrane fluidity studies in intact living cells. TMA-DPH (in blue) locates near the polar heads of phospholipids; anionic phospholipids are represented in red and zwitterionic in yellow (125). (Adapted from Ribeiro, M., *et al. Frontiers in Cellular Neuroscience*. 2012, 6: 1-7.)

## CHAPTER II

### EVALUATING MEMBRANE FLUIDITY USING TIME-CORRELATED SINGLE PHOTON COUNTING FLUORESCENCE ANISOTROPY

#### INTRODUCTION

As previously established, IR's function best when clustered in specific microdomains within the plasma membrane and are influenced by the lipid packing of the plasma membrane. Changes in the fluidity of the PM would imply changes in the lipid packing of the cell. The goal of this project is to investigate the effect on the PM of BMOV treatment in the plasma membrane of RBL-2H3 cells. In order to measure membrane fluidity we will use time-correlated, single photon counting fluorescence anisotropy.

RBL-2H3 cells are well characterized and have well characterized PM's, specifically with Type 1 Fcε receptors. Multiple studies have described Type 1 Fcε receptor's lateral dynamics and signaling within membrane MDs. Like the IR, proper signaling requires positioning within a MD. (126-130). Therefore RBL-2H3 cells were selected for experimentation.

#### MATERIALS

Minimum Essential Medium (MEM) with Earle's Balanced Salts was purchased from Thermo Scientific (Logan, Utah). Fetal bovine serum (FBS) was purchased from Invitrogen (Carlsbad, CA). L-glutamine, penicillin and streptomycin and amphotericin B, (PSA) were purchased from Gemini BioProducts (Woodland, CA). Insulin from bovine pancreas was purchased from Sigma-Aldrich (St. Louis, MO). BMOV and oxidized BMOV were synthesized and characterized as previously described (131-132). For cell experiments, BMOV was prepared fresh before each experiment as a 100x stock solution in phosphate buffered saline (PBS), pH 7.2,

by the Crans laboratory. TMA-DPH and Trypan blue were purchased from Molecular Probes Invitrogen (Grand Island, NY). Ficoll, and EDTA were purchased from Sigma Aldrich, (St. Louis, MO). NaOH and HCl were purchased from Fisher Scientific (Denver, CO). Doubly distilled deionized water with specific resistivity  $\geq 17.8 \text{ M}\Omega\cdot\text{cm}$  (Barnstead E-pure system) was used throughout. Eppendorf 2mL tubes were purchased from Sigma Aldrich, (Milwaukee, WI). BD Falcon 75mL polystyrene sterile non-pyrogenic flasks and BD Falcon 50mL polypropylene conical tubes were purchased from BD Biosciences, (San Jose, CA). 10mm Quartz Fluorometer cuvettes were purchased from Starna Cells (Atascadero, CA). Hemacytometer was purchased from Beckman Coulter, (Brea, CA) RBL-2H3 cells were kindly provided by Dr. Reuben Siraganian of the National Institutes of Health. Instrumentation includes the Jobin IBH Model 500F with Xenon Flashlamp Fluorometer and LUDOX were purchased from Jobin Yvon IBH (Glasgow, UK). The Zeiss Axiomat microscope equipped with a Zeiss 63x NA 1.2, Plan Neofluar immersion fluorescence objective with appropriate Omega dichroic mirrors and filters for imaging TMA-DPH fluorescence were purchased from Zeiss (Germany). The Damon/IEC DPR-6000 Centrifuge was purchased from Thermo Scientific (Asheville, NC). Data analysis was performed using Microsoft Excel.

## METHODS

### *Cell Culture*

RBL-2H3 cells were maintained in RBL-2H3 medium made of 830mL MEM, 150mL FBS, 10mL PSA, 10mL L-glutamine which was sterilized via vacuum filtration filter. For serum starving cells, a medium was prepared with only 980mL MEM, 10mL and PSA, 10mL L-

glutamine. Cells were incubated in ThermoForma Series II Water Jacketed CO<sub>2</sub> Incubator with Hepa filter at 37°C, 5%CO<sub>2</sub> and grown to 90% confluency.

### *Cell Counting Protocol*

Cells were serum starved overnight. Control cells were not serum starved. At 16hrs, cells were removed from the incubator. The medium was removed and discarded and replaced with 8mM EDTA (pH 8.0) in 1X PBS to remove cells from the flask. Cells were washed with 5mL 1X PBS and transferred to 50mL conical centrifuge tubes. Cell samples were spun at 1000 RPM for 3 minutes. Supernatant was discarded and pellet was suspended in 10mL 1X PBS. This cycle was repeated 3 times. After last spin, supernatant as discarded and pellet was suspended in 1xPBS to equal exactly 1mL. In an Eppendorf tube, 10μL of cells from the 1mL suspended pellet solution was placed and 990μL 1X PBS, and 1mL Trypan blue was added. The Eppendorf tube was briefly agitated to insure distribution of the Trypan blue dye. A Beckman Hemacytometer was loaded with 10μL Trypan blue cell mixture on each side and cells imaged under microscopy. Cell viability of 95% was the requirement for continuing with anisotropy measurements (124).

### *Instrument Parameters for Anisotropy Measurements*

The Jovin IBH Fluorometer was programmed with a prompt excitation at 372nm, a prompt excitation monochromator of 372nm, and emissions monochromator of 435nm. These are within the 20nm range of the maximum absorption and emission of the membrane probe TMA-DPH. Excitation was provided by a 372nm Nano-LED light source. The slit width was set to the widest setting at 32nm. This was done to decrease the timeframe required to collect

10,000 counts. Polarizers were programmed to collect data in the following positions: vertical-vertical (V-V), vertical-horizontal (V-H), horizontal-horizontal (H-H), and horizontal-vertical (H-V). These orientations are required in order to calculate the anisotropy value for a sample based on Equation 1 and Equation 3 in Chapter I in the section on TCSPC Anisotropy. A solution of LUDOX specific for the IBH was used to zero the instrument to subtract light scatter. After initial data was collected, a short pass filter at 390nm was added and used on all subsequent experiments. (See Results section Figure 13). All data were analyzed and figures were created using a Microsoft Excel program.

### *Treatments*

Please refer to Table 1 for experimental design. Treated cells were incubated with BMOV 1 hour prior to imaging in concentrations ranging from 10 $\mu$ M to 0.1 $\mu$ M, and/or 200nM insulin. The fluorescent membrane probe, TMA-DPH, was applied in a 10 $\mu$ M concentration 10 minutes prior to imaging. Cells were then harvested and counted via the cell counting protocol below. Cells were then imaged in a 9% Ficoll solution in 10mm quartz cuvettes at a concentration of 1x10<sup>6</sup> cells/mL. Control cells were only treated with 10 $\mu$ M TMA-DPH. Within separate flasks, cells were labeled controls and for each treatment applied. These flasks were imaged using the Zeiss Axiomat microscope in order to assess the health of the cells during the timeframe of data collection using the IBH Fluorometer on prepared cell samples.

Table 1. Experimental Design.

	CONTROL 1	Experiment 1 A	Experiment 1 B	Experiment 1 C
Cells	RBL-2H3	RBL-2H3	RBL-2H3	RBL-2H3
Medium	Standard	Serum Starved	Serum Starved	Serum Starved
10 $\mu$ M TMA-DPH	+	+	+	+
9%Ficoll	+	+	+	+
10 $\mu$ M BMOV	∅	+	∅	+
200nM Insulin	∅	∅	+	+
	CONTROL 2	Experiment 2 A	Experiment 2 B	Experiment 2 C
Cells	RBL-2H3	RBL-2H3	RBL-2H3	RBL-2H3
Medium	Standard	Serum Starved	Serum Starved	Serum Starved
10 $\mu$ M TMA-DPH	+	+	+	+
9%Ficoll	+	+	+	+
1 $\mu$ M BMOV	∅	+	∅	+
200nM Insulin	∅	∅	+	+
	CONTROL 3	Experiment 3 A	Experiment 3 B	Experiment 3 C
Cells	RBL-2H3	RBL-2H3	RBL-2H3	RBL-2H3
Medium	Standard	Serum Starved	Serum Starved	Serum Starved
10 $\mu$ M TMA-DPH	+	+	+	+
9%Ficoll	+	+	+	+
0.1 $\mu$ M BMOV	∅	+	∅	+
200nM Insulin	∅	∅	+	+

## RESULTS

Addition of a short pass filter to the IBH apparatus for anisotropy measurements resulted in anisotropy values that were closer to the theoretical maximum allowed of 0.4 as seen in Figure 13.

In Figure 14, 200nM insulin caused an increase in anisotropy compared to untreated cells. 10 $\mu$ M BMOV treated cells had a larger increase in anisotropy than when the cells were incubated with 10 $\mu$ M BMOV and 200nM insulin, but less than cells treated with insulin alone.

In Figure 15, 200nM insulin again caused the largest increase in anisotropy compared to untreated cells. 1 $\mu$ M BMOV treated cells again had an increase in anisotropy compared to untreated cells, but had less effect than 200nM insulin. 1 $\mu$ M BMOV and 200nM insulin caused decreased anisotropy compared to untreated cells.

In Figure 16, the largest increase in anisotropy was seen in 0.1 $\mu$ M BMOV compared to untreated cells. Cells treated with 200nM insulin also demonstrated an increase in anisotropy over untreated cells but this was less than the effect of 0.1 $\mu$ M BMOV. Cells treated with 0.1 $\mu$ M BMOV and 200nM insulin showed an increase in anisotropy over untreated cells but less than cells treated with either BMOV or insulin alone.

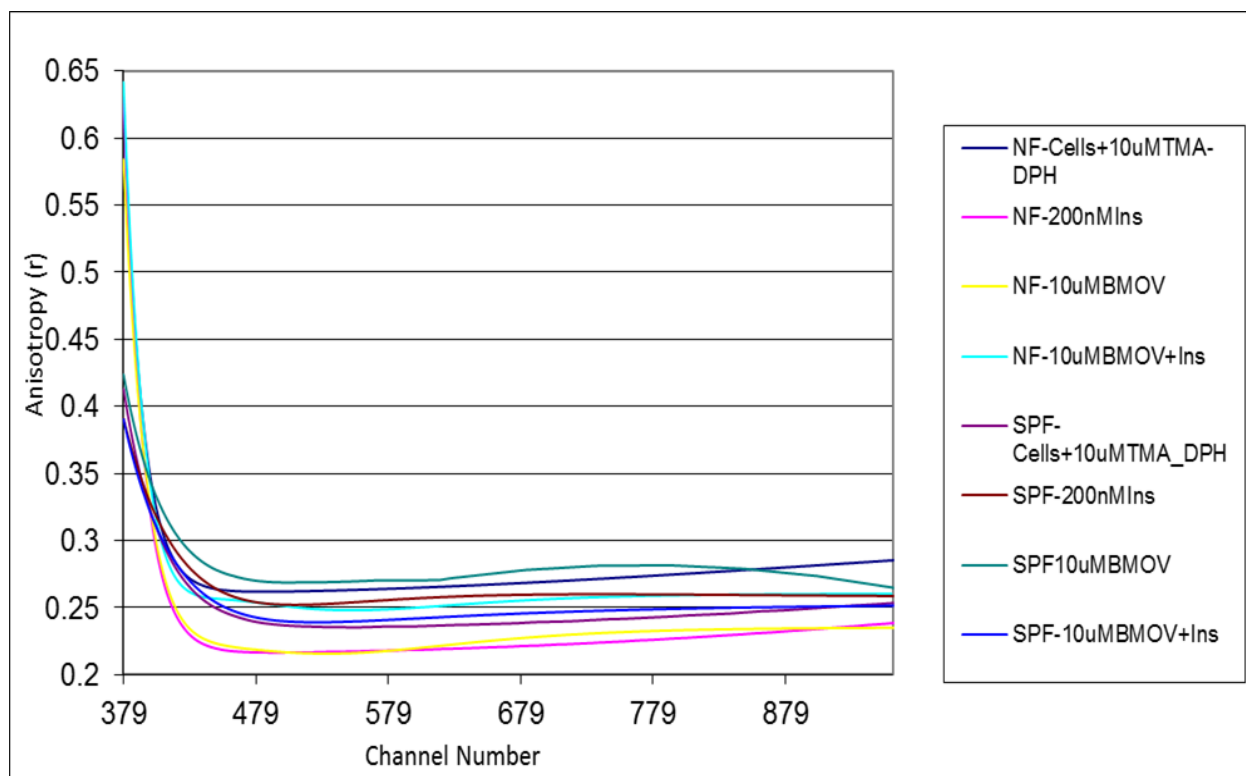


Figure 13. The effect of a 390nm short pass filter on TCSPC anisotropy measurements on RBL-2H3 cells. The y-axis is anisotropy ( $r$ ), and the x-axis is channel number. Measurements were done until 10,000 counts of data had been collected. NF indicates no filter was used in the measurements. SPF indicates that the 390nm short pass filter was used in the measurements.

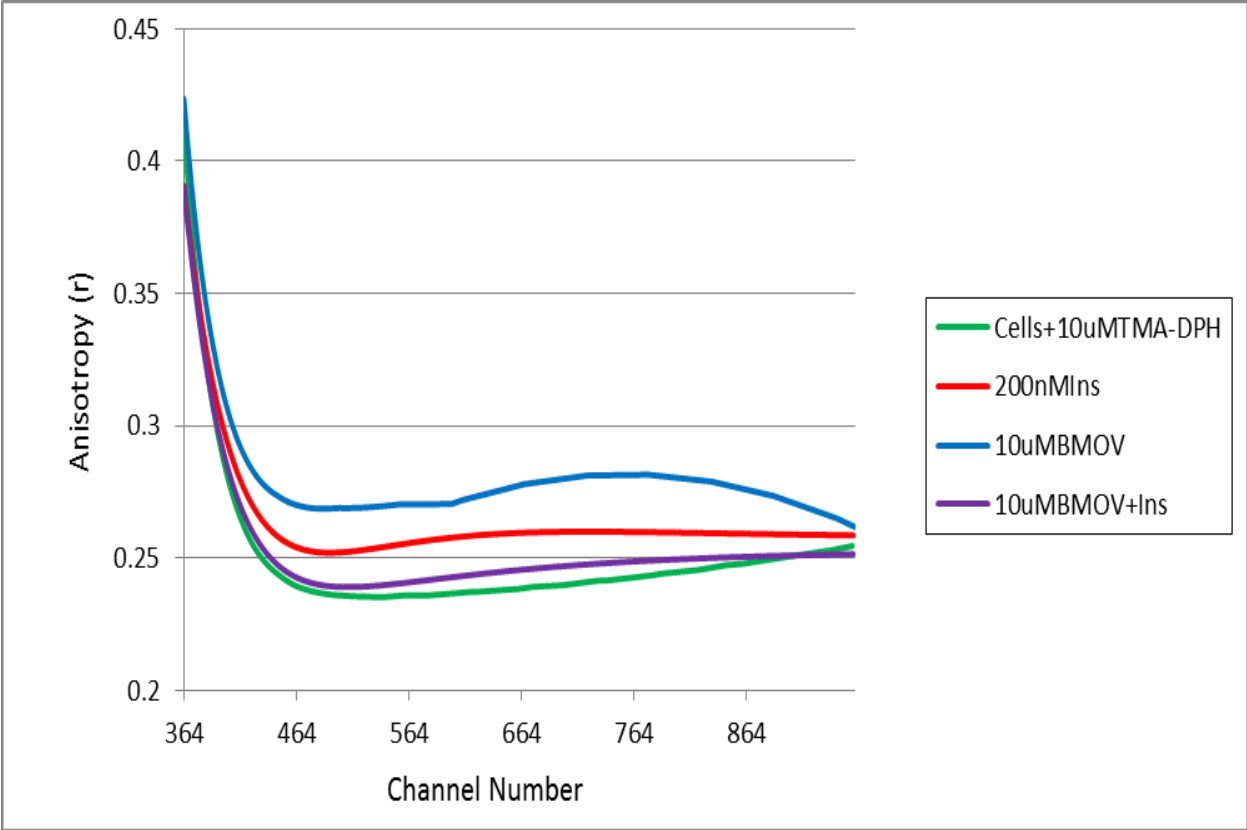


Figure 14. Experiment 1. TCSPC Anisotropies of RBL-2H3 cells labeled with 10 $\mu$ M TMA-DPH and treated with 10 $\mu$ M BMOV, 10 $\mu$ M BMOV and 200nM insulin, and 200nM alone.

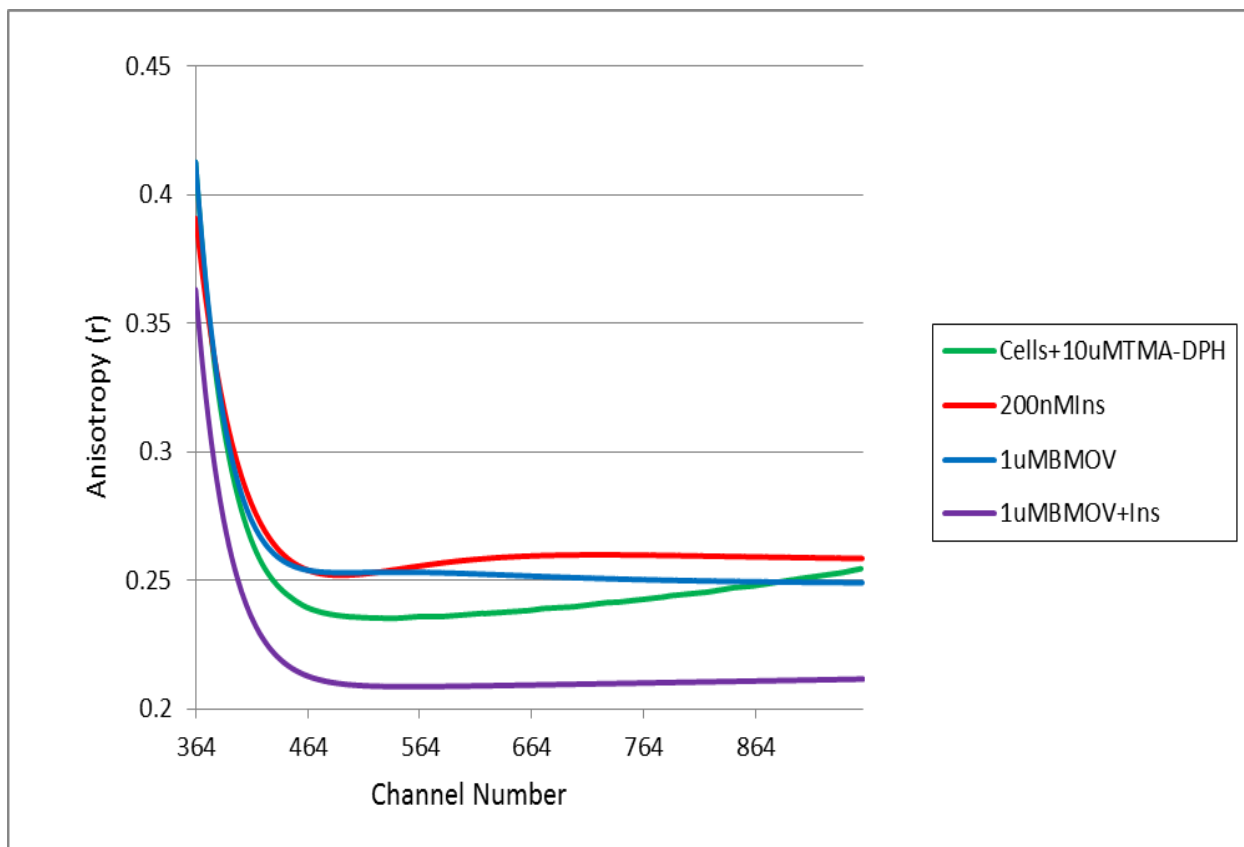


Figure 15. Experiment 2. TCSPC Anisotropies of RBL-2H3 cells labeled with 10 $\mu$ M TMA-DPH and treated with 1 $\mu$ M BMOV, 1 $\mu$ M BMOV and 200nM insulin, and 200nM insulin alone.

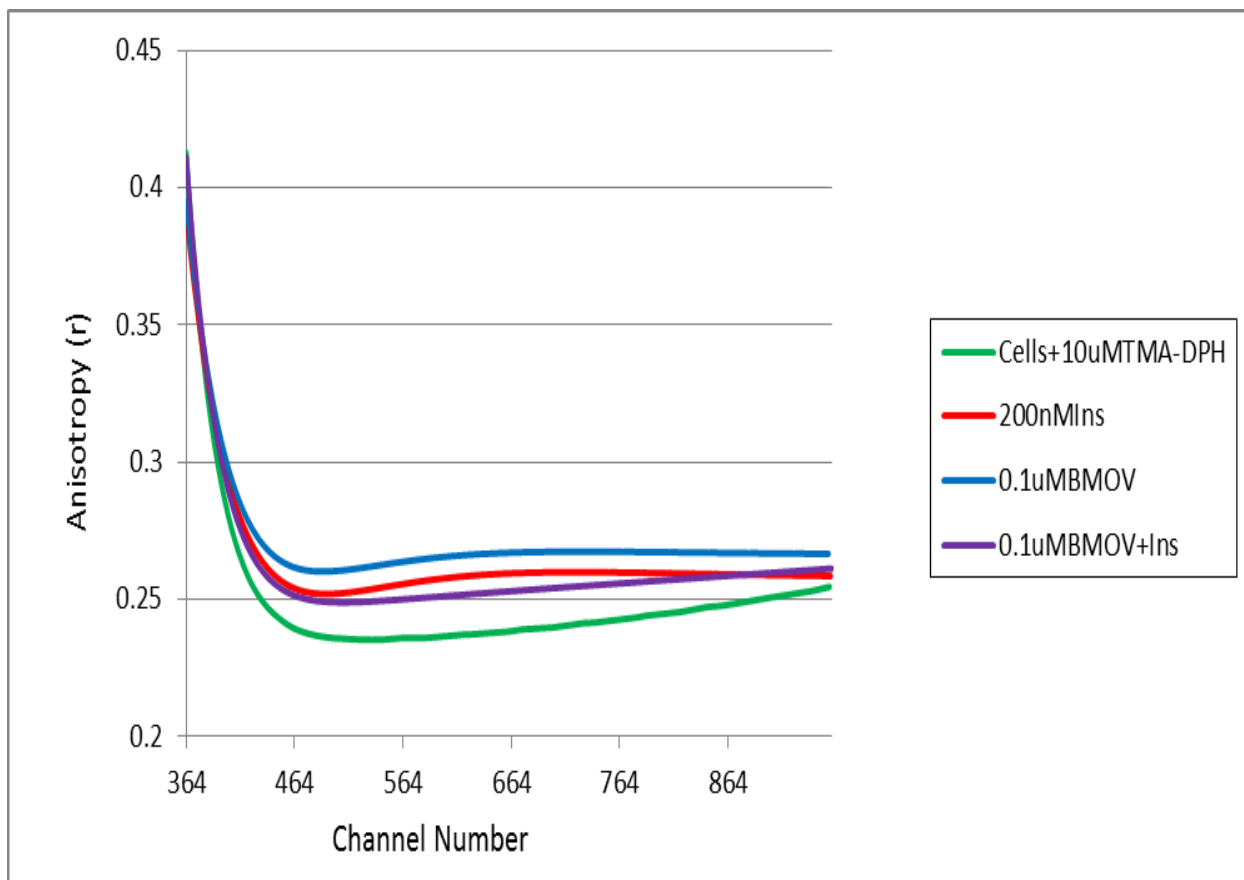


Figure 16. Experiment 3. TCSPC Anisotropies of RBL-2H3 cells labeled with 10 $\mu$ M TMA-DPH and treated with 0.1 $\mu$ M BMOV, 0.1 $\mu$ M BMOV and 200nM insulin, and 200nM insulin alone.

## DISCUSSION

When first developing the method for measuring membrane fluidity in RBL-2H3 cells, a number of challenges arose. Early in the development of this method using the IBH, we found that cells would begin to precipitate in solution. To rectify this problem Ficoll was added to equal 9% of the cell solution. Ficoll was chosen after absorption and emission spectra demonstrated that it does not absorb or emit within the spectrum of TMA-DPH (data not shown). The use of Ficoll kept the cells suspended for the duration of the experiments.

When analyzing the data from Figure 13, it is clear that there is a noticeable decrease in the maximal anisotropy with the addition of the 390nm short pass filter. This filter was added to the IBH apparatus with the sole purpose of decreasing the amount of scattered light and cross-talk that can occur in the fluorescing samples. Given the improvement in the measurements following the addition of the short pass filter, it was included for the rest of the anisotropy measurements carried out on the cells.

It is clear when looking at Figures 14-16 that there is a lack of consistency between each of the experiments as to which treatment resulted in the greatest increase in anisotropy. An increase in anisotropy should correlate to a decrease in membrane fluidity due to an increase in lipid packing. In Figures 14 and 15, 200nM insulin caused the greatest decrease in membrane fluidity, but in Figure 16 this treatment did not demonstrate the same effect. Also of note, is that there was a marked decrease in anisotropy in Figure 15 in cells treated with both 0.1 $\mu$ M BMOV and 200nM insulin. This would indicate that cells treated with 0.1 $\mu$ M BMOV + 200nM insulin actually resulted in an increase in membrane fluidity which would correlate with a loss of lipid packing.

To explain the inconsistencies found in the above data, the cells that were left plated on the flasks but treated with the same treatments as those placed in the cuvettes for measurement in the IBH were imaged. It was found that during the timeframe of the experiments, the cells were not able to maintain the 95% viability. Cells began to show blebbing of their membranes which indicated cell stress and apoptosis. In some flasks, cells had completely lost adhesion to the floor of the flasks and floated in the medium. Samples from these flasks were taken and the cell counting protocol was performed. Viable cells in these samples ranged from 10%-30% (data not

shown). The loss of membrane integrity is the mostly explanation for the inconsistencies in the data.

Concern for the viability of the cells was first raised when the first rounds of experiments were requiring hours of time to collect the 10,000 counts of photons set as our initial parameters. Steps were taken to optimize the parameters on the IBH and decrease the time needed to acquire 10,000 counts. However, prior to being able to decrease the timeframe of experiments, cells were reserved to be treated and observed under microscopy to evaluate viability. It was also found that not only did the cell membrane integrity begin to fail as the viability of the cells decreased, but some samples demonstrated internalization of the TMA-DPH intracellularly (data not shown). It was not clear whether this was a diffusive process, a loss of membrane integrity, or part of membrane cycling.

## CONCLUSIONS AND FUTURE DIRECTIONS

Given the difficulties encountered with the cells due to the timescale of the experiments, it might be more advantageous to explore other methods of collecting membrane fluidity measurements. One option is ratiometric imaging of a specific fluorophore such as Di-4-ANEPPDHQ, which has a change in emission based on membrane lipid packing. For example, its fluorescence emission is red at 605nm when the probe is restricted, but emission is green at 530 nm when there is an increase in the viscosity of the probe's environment. This probe could potentially decrease the time required to collect data, thereby increasing the likelihood that the cells would still be living at the end of the experiments. This would obviously allow for a more definitive discussion of the data and implications drawn from the data collected.

Other options exist for fluorophores to probe the PM. These include Di-I C-18, PE, PC, DPH, and Di-O with each demonstrating an affinity for a specific portion of the membrane. Some preferentially stay in the hydrophobic section of the PM bilayer. Others prefer either the cytoplasmic or extracellular leaflets of the membrane. It would be of interest whether BMOV or other transition metal compounds specifically affect specialized membrane regions identified by these various probes.

All of the experiments were performed at 25°C. Physiologic temperature is 37°C. For completeness, measurements at 4°, 15°, 25°, and 37°C should be completed. Measurements at 4°C were attempted but at this temperature, the lines carrying the cold water from the ice bath to the housing holding the cuvettes froze and the temperature was not maintained even with insulation of water lines.

As lipid peroxidation has been demonstrated to affect the insulin molecule, it would be interesting to know if the products of lipid peroxidation also affect the IR itself or its location in lipid raft fractions. This could be done using a discontinuous sucrose gradient after treating cells with the oxidizing molecules described by Navarro and Pillon *et al.* (73,74). Along these same lines, changes in the IR or the IR localization in response to exposure with the lipid peroxidation products is of interest as are effects of treatment with BMOV and other transition metals on the modified IR or lipid raft localization, or on the modified insulin molecule itself.

Given that ceramide is an intermediate for sphingomyelin degradation, it would be interesting to know what effect the lipid peroxidation products discussed above had on ceramide levels in treated and untreated cells and what effect, if any, BMOV and other transition metals had on ceramide levels.

Various compounds have demonstrated redox chemistry once the vanadium compounds reach the cell as well as during transport through the body. Investigation of the potential for redox reactions between lipid peroxidation products and vanadium species would be prudent. Such a mechanism would explain lipid and glucose normalization properties of some vanadium complexes.

Of note is the link between the metabolic derangements discussed and fertility, specifically with respect to Polycystic Ovarian Syndrome (PCOS). Patients with this syndrome typically have obesity, insulin resistance, hirsutism, elevated levels of aldosterone, irregular menses, and issues with infertility. The relationship between increased aldosterone levels and insulin resistance has not been elucidated (133). It would be interesting to see if BMOV or other transition metal compounds are able to affect aldosterone production, or if they exert an effect on other hormones regulating the menstrual cycle such as estrogen, follicle stimulating hormone

(FSH) and luteinizing hormone (LH). It would also be interesting to know if there is any change in the aldosterone molecule secondary to the effects of ROS or toxic metabolites of PM lipid peroxidation as described in the insulin molecule by Navarro and Pillon (73,74).

All of the above experiments would be performed on RBL-2H3 cells. It would also be prudent to know how adipocytes, specifically 3T3-L1 adipocytes, which have been well characterized, respond to treatment with vanadium and other transition metal compounds. For experiments investigating transition metal compounds and PCOS, in addition to adipocytes, theca and granulosa cells would be appropriate.

## REFERENCES

1. Taylor, R. N. *Engl. J. Med.*, 2004, 7: 639-641.
2. Yanovski, S. Z.; Yanovski, J. A.; *N. Engl. J. Med.* 2002, 346: 591-602.
3. Olshansky, S. J.; Passaro, D. J.; Hershow, R. C.; Layden, J.; Carnes, B. A.; Brody, J.; Hayflick, L.; Butler, R. N.; Allison, D. B.; Ludwig, D. S. N. *Engl. J. Med.* 2005, 352: 1138-1145.
4. Flegal, K. M., Kit, B. K., Orpana, H., Graubard, B. I. *JAMA*, 2013, 309:71-82.
5. Trayhurn, P. and Wood, I. S., *Br. J. Nutr.*, 2004, 92: 347.
6. Kahn, B. B. and Flier, J. S., *J. Clin. Invest.*, 2000, 106: 473.
7. Cavaghan, M. K., Ehrmann, D. A., Polonsky, K. S., *J. Clin. Invest.*, 2000, 106: 329.
8. Smyth, S.; Heron, A.; *Nat. Med.* 2006, 12: 75-80.
9. Montecucco, F.; Steffens, S.; Mach, F. *Mediators Inflamm* 2008, 2008: 1-10.
10. Cimbaljevic, B.; Vasiljevic, A.; Cimbaljevic, S.; Buzadzic, B.; Korac, A.; Petrovic, V.; Jankovic, A.; Korac, B. *Can. J. Physiol. Pharmacol.* 2007, 85: 997-1003.
11. Eckel R. H, Kahn R, Robertson R. M., Rizza R. A., *Circulation.* 2006;113(25):2943.
12. Grundy, S. M., *J Clin Endocrinol Metab.* 2007;92(2):399.
13. Rosenzweig, J. L., Ferrannini, E., Grundy, S. M., Haffner, S. M., Heine, R. J., Horton, E. S., Kawamori, R., Endocrine Society *J Clin Endocrinol Metab.* 2008;93(10):3671.
14. Grundy, S. M., Cleeman, J. I., Daniels, S. R., Donato, K. A., Eckel, R. H., Franklin, B. A., Gordon, D. J., Krauss, R. M., Savage, P. J., Smith, S. C. Jr, Spertus, J. A., Costa, F., American Heart Association, National Heart, Lung, and Blood Institute, *Circulation.* 2005;112(17):2735.
15. Grundy SM, Hansen B, Smith SC Jr, Cleeman JI, Kahn RA, American Heart Association, National Heart, Lung, and Blood Institute, American Diabetes Association, *Circulation.* 2004;109(4):551.
16. Saltiel, A. R.; Pessin, J. E. *Trends in Cell Bio*, 2002, 12, 65-71.
17. Owens, D., *Nature Reviews*, 2002, 1:529-540.

18. Kido, Y.; Nakae, J.; Accili, D. *J. Clinical Endocrinology and Metabolism*, 2001, 86, 972-979.
19. Lee, J.; Pilch, P. F. *Am. J. Physiol*, 1994, 35, 319-334.
20. De Meyts, P., and Whittaker, J. *Nature Reviews*, 2002, 1: 769-783.
21. White, M.F. *Mol. Cell. Biochem*, 1998, 182, 3-11.
22. Alessi, D. R.; Deak, M. ; Cassamayor, A. ; Caudwell, F. B.; Morrice, N.; Norman, D. G.; Gaffney, R.; Reese, C. B.; MacDougall, C.N.; Harbison, D.; Ashworth, A.; Bownes, M. *Curr Bio*, 1997, 7, 776-789.
23. Saltiel, A. R.; Kahn, C. R. *Nature*, 2001, 414: 799-806.
24. Vollenweider, P. *Mol. Cell. Bio.*, 1999, 19, 1081-1091.
25. Koricanac, G.; Isenovic, E.; Stojanovic-Susulic, V.; Miskovic, D.; Zakula, Z.; Ribarac-Stepic, N. *Gen. Physiol. Biochem.* 2005, 25, 11-24.
26. Dey, D.; Mukherjee, M.; Basu, D.; Datta, M.; Roy, S. S.; Bandyopadhyay, A.; Bhattacharya, S. *Cell. Physiol. Biochem.* 2005, 16, 217-228.
27. Hegarty, B. D.; Bobard, A.; Hainault, I.; Ferre, P.; Bossard, P.; Foufelle, F. P. *Natl. Acad. Sci.* 2005, 102, 791-796.
28. Vainio, S.; Heino, S.; Mansson, J. E.; Fredman, P.; Kuismanen, E.; Vaarala, Q.; Ikonen, E. *EMBO Reports*, 2002, 15, 95-100.
29. Simons, K.; Toomre, D. *Molecular Cell Biology*, 2000, 1, 31-41.
30. Gustavsson, J.; Parpal, S.; Karlsson, M.; Ramsing, C.; Thorn, H.; Borg, M.; Lindroth, M.; Peterson, K. H.; Magnusson, K. E.; Stralfors, P. *FASEB*, 1999, 13: 1961-1971.
31. Kabayama, K.; Sato, T.; Kitamura, F.; Uemar, S.; Kang, B.W.; Igarashi, Y.; Inokuchi, J. *Glycobiology*, 2005, 15: 21-29.
32. Scherer, P. E.; Lisanti, M. P.; Baldini, G.; Sargiacomo, M.; Mastick, C. C.; Lodish, H. F. *J. Cell Bio.*, 1994, 127: 1233-1243.
33. Anderson, R. G. *Proc. Natl. Acad. Sci. USA*, 1993, 90: 10909-10913.
34. Parpal, S.; Karlsson, M.; Thorn, H.; Stralfors, P. *J. Bio. Chem.*, 2001, 276: 9670-9678.
35. Singer, S. J., Nicolson, G. L., *Science*, 1972, 175:720-731.

36. Pomorski, T., Holthuis, J. C. M., Herman, A., van Meer, G., *J. Cell Sci.* 2004, 117: 80-813.
37. Daleke, D. L., *J. Lipid Res.* 2003, 44: 233-242.
38. Menon, A. K., Watkins, W. E., Hrafnisdottir, S., *Curr. Biol.* 2000, 10: 241-252.
39. Bretscher, M. S. *Nat. New Biol.* 1972, 236: 11-12.
40. Pietzsch, J., Horizon Symposia: Living Frontier, *Nature*, 2004, 1-4.
41. Daleke, D. L., *J. Biol. Chem.* 2006, 282: 821-825.
42. Bishop, W. R., and Bell, R. M., *Cell* 1985, 42: 51-60.
43. Buton, X., Morrot, G., Fellmann, P., Seigneuret, M., *J. Biol. Chem.* 1996, 271: 6651-6657.
44. Nicholson, T. and Mayinger, P., *FEBS Lett.* 2000, 476: 277-281.
45. Brown, D. A. and London, E. *Annu. Rev. Cell Dev. Bio.* 1998, 14: 111.
46. Edidin, M. *Annu. Rev. Biophys. Biomol. Struct.* 2003, 32: 257.
47. Simons, K. and Ikonen, E. *Nature* 1997, 387: 569.
48. Hancock, J. F., *Nat. Rev. Mol. Cell Biol.* 2006, 7: 456.
49. Semrau, S., and Schmidt, T., *Soft Matter, J. Royal. Soc. Chem.* 2009, 5: 3174-3186.
50. Liu, G.; Kleine, L.; Hebert, R. L. *Critical Reviews in clinical Laboratory Sciences*, 1999, 36: 511-573.
51. Holland, W. L.; Summers, S. A. *Endocrine Reviews*, 2008, 4: 381-402.
52. Hannun, Y. A.; Oeide, L. M. *Molecular Cell Biology* 2008, 9: 139-150.
53. Hait, N. C.; Osteritzian, C. A.; Paugh, S. W.; Milstein, S.; Spiegel, S. *Biochim Biophys Acta* 2006, 1758: 2016-2026.
54. Wymann, M. P.; Schneiter, R. *Molecular Cell Biology*, 2008, 9: 162-176.
55. *Inflammation and lipid peroxidation pathway*. Digital Image. Merck Biosciences. United Kingdom, n.d. Web. 02 July 2009. <[www.merckbiosciences.com.uk](http://www.merckbiosciences.com.uk)>.

56. Cardona, F.; Tunez, I.; Tasset, I.; Montilla, P.; Collantes, E.; Tinahones, F. J. *Euro J Clin Invest* 2008, 38: 510-515.
57. Kabayama, K.; Sato, T.; Kitamura, F.; Uemar, S.; Kang, B.W.; Igarashi, Y.; Inokuchi, J. *Glycobiology* 2005, 15: 21-29.
58. Steinburg, G. R.; Michell, B. J.; van Denderen, B. J.; Watt, M. J.; Carey, A. L.; Fam, B. C.; Andrikopoulos, A.; Proietto, J.; Gorgun, C. Z.; Carling, D.; Hotamisligil, G. S.; Febbraio, M. A.; Kay, T. W.; Kemp, B. E. *Cell Metab* 2006, 4: 465-474.
59. Dyck, D. J.; Heigenhauser, G. J.; Bruce, C. R. *Acta Physiol* 2006, 186: 5-16.
60. Bruce, C. R.; Dyck, D. J. *Am J Physiol Endocrinol Metab* 2004, 287: E616-E621.
61. Zeidan, Y. H.; Jenkins, R. W.; Hannun, Y. A. *J Cell Bio* 2008, 181: 335-350.
62. Le Marchand-Brustel, Y.; Gaul, P.; Gremeaux, T.; Gonzalez, T.; Barres, R.; Tanti, J. F. *Biochemical Society Transactions*, 2003, 31: 1152-1156.
63. Smyth, S.; Heron, A.; *Nat. Med.* 2006, 12: 75-80.
64. Boord, J. B.; Maeda, K.; Makowski, L.; Babaev, V.; Fazio, S.; Linton, M. F.; Hotamisligil, G. *Circulation*. 2004, 110:1492-1498.
65. Furuhashi, M.; Fucho, R.; Gorgun, C. Z.; Tuncman, G.; Cao, H.; Hotamisligil, G. *J. Clin. Invest.* 2008, 7: 2640-2650.
66. Tas, S.; Sarandol, E.; Ayvalik, S. Z.; Serdar, Z.; Dirican, M. *Archives of Medical Research* 2007, 38: 276-283.
67. Cardona, F.; Tunez, I.; Tasset, I.; Murri, M.; Tinahones, F. J. *Clinical Biochemistry* 2008, 41: 701-705.
68. Rucich, A.; Tiroshi, A.; Potashnick, R.; Hemi, R.; Kanety, H.; Bashan, N. *Diabetes* 1998, 47: 1562-1569.
69. Maddux, B. A.; See, W.; Lawrence Jr, J. C.; Goldfine, A. L.; Goldfine, I. D.; Evans, J. L. *Diabetes* 2001, 50: 404-410.
70. Ramakrishna, V.; Jaiikhani, R. *Acta Diabetol* 2008, 45: 41-46.
71. Puri, V.; Ranjit, S.; Konda, S.; Nicoloro, S.; Straubhaar, J.; Charla, A.; Chouinard, M.; Lin, C.; Buckart, A.; Corvera, S.; Perugini, R. A.; Czech, M. P. *PNAS* 2008, 105: 7833-7838.
72. Lei, X. G.; Cheng, W. H.; McClung, J. P. *Annual Review of Nutrition* 2007, 27: 41-61.

73. Pillon, N. J., Vella, R. E., Soulere, L., Becchi, M., Lagarde, M., Soulage, C. O., *Chemical Research in Toxicology* 2011, 24: 752-762.
74. Navarro, N. M., Guzman-Grenfell, A. M., Olivares-Corichi, I., Hicks, J. J. In *Advanced Protocols in Oxidative Stress II: Methods in Molecular Biology*, Armstrong, D., Ed. Humana Press of Springer, 2010, Berlin, Germany, p 141-153.
75. Lyonette, M. and E. Martin. *La Presse Medicale* 1889, 32:191-192.)
76. Shechter, Y.; Karlsh, S. J. D. *Nature* 1980, 284, 556-558.
77. Shechter, Y.; Meyerovitch, J.; Farfel, Z.; Sack, J.; Bruck, R.; Bar-Meir, S.; Amir, S.; Degani, H.; Karlsh, S. J. D. In *Vanadium in Biological Systems: Physiology and Biochemistry*; Chasteen, N. D., Ed.; Kluwer Academic Publishers: Boston, 1990, p 129-142.
78. Michibata, H.; Sakurai, H. In *Vanadium in Biological Systems: Physiology and Biochemistry*; Chasteen, N. D., Ed.; Kluwer Academic Publishers: Boston, 1990, p 153-172.
79. Sakurai, H.; Tamura, A.; Fugono, J.; Yasui, H.; Kiss, T. *Coord. Chem. Rev.* 2003, 245, 31-37.
80. Crans, D. C.; Smee, J. J.; Gaidamauskas, E.; Yang, L. *Chem. Rev.* 2004, 104, 849-902.
81. Thompson, K. H.; and Orvig, C. *Dalton Trans.* 2006, 761-764.
82. Anderson, R. A., *Diabetes Metabol* 2000, 26:22-27.
83. Clodfelder, B. J., Upchurch, R. G., Vincent, J. B., *J. Inorg. Biochem* 2004, 98:522-33.
84. Ozcelikay, A.T., Becker, D. J., Ongemba, L. N., Pottier, A. M., Henquin, J. C., Brichard, S. M., *J. Am. J. Physiol.* 1996, 270:E344-52.
85. Brautigan, D. L., Kruszewski, A., Wang, H. *Biochem. Biophys. Res. Commun.* 2006, 347:769-773.
86. Thompson, K.H., Chiles, J., Yuen, V. G., Tse, J., McNeill, J. H., Orvig, C. *J. Inorg. Biochem.* 2004, 98:683-90.
87. Willsky, G. R.; Chi, L.-H.; Liang, Y.; Gaile, D. P.; Hu, Z.; Crans, D. C. *Physiol. Genomics* 2006, 26, 192-201.
88. Basuki, W.; Hiromura, M.; Adachi, Y.; Tayama, K.; Hattori, M.; Sakurai, H. *Biochem. Bioph. Res. Co.* 2006, 349, 1163-1170.

89. Shechter, Y.; Goldwaser, I.; Mironchik, M.; Fridkin, M.; Gefel, D. *Coord. Chem. Rev.* 2003, 237, 3-11.
90. Liboiron, B. D.; Thompson, K. H.; Hanson, G. R.; Lam, E.; Aebischer, N.; Orvig, C. *J. Am. Chem. Soc.* 2005, 127, 5104-5115.
91. Shechter, Y., Goldwaser, I., Mironchik, M., Fridkin, M., Gefel, D., *Coord. Chem. Rev.* 2003, 237, 3-11.
92. Yuan, C. X., Lu, L. P., Gao, X. L., Wu, Y. B., Guo, M. L., Li, Y., Fu, X. Q., Zhu, M. L., *J. Biol. Inorg. Chem.* 2009, 14, 841-851.
93. Huyer, G., Liu, S., Kelly, J., Moffat, J., Payette, P. Kennedy, B., Tsaprailis, G., Gresser, M. J., Ramachandran, C., *J. Biol. Chem.* 1997, 272, 843-851.
94. Posner, B. I., Faure, R., Burgess, J. W., Bevan, A. P., Lachance, D., Zhang-Sun, G., Fantus, I. G., Ng, J. B., Hall, D. A., Lum, B. S., Shaver, A. *J. Biol. Chem.* 1994, 269, 4596-4604.
95. Li, M., Ding, W., Baruah, B., Crans, D. C., Wang, R., *J. Inorg. Biochem.*, 2008, 102, 1846-1853.
96. Tracey, A. S., *J. Inorg. Biochem.* 2000, 80: 11-16.
97. Bhattacharyya, S. A., Martinsson, R. J., Batchelor, R. J., Einstein, F. W. B., Tracey, A. S., *Can. J. Chem.* 2001, 79: 938-948.
98. Bhattacharyya, S. A. and Tracey, A. S., *J. Inorg. Biochem.* 2001. 85: 9-13.
99. Elberg, G., He, Z., Li, J., Sekar, N., Shechter, Y., *Diabetes*, 1997, 46: 1648-1690.
100. Ou, H., Yan, L., Mustafi, D., Makinen, M., Brady, M. J., *J. Biolog. Inorg. Chem.* 2005, 10: 874-886.
101. Buglyo, P.; Crans, D. C.; Nagy, E. M.; Lindo, R. L.; Yang, L.; Smee, J. J.; Jin, W.; Chi, L.-H.; Godzala, M. E.; Willsky, G. R. *Inorg. Chem.* 2005, 44: 5416-5427.
102. Monga, V.; Thompson, K. H.; Yuen, V. G.; Sharma, V.; Patrick, B. O.; McNeill, J. H.; Orvig, C. *Inorg. Chem.* 2005, 44: 2678-2688.
103. Sakurai, H.; Kawabe, K.; Yasui, H.; Kojima, Y.; Yoshikawa, Y. *J. Inorg. Biochem.* 2001, 86, 94-94.
104. Barrand, M. A., Callinham, B. A., Hider, R. C., *J. Pharm. Pharmacol.* 1987, 39: 203-211.
105. Morinville, A., Maysinger, D., Shaver, A., *Trends Pharmacol. Sci.* 1998, 19: 452-460.

106. Sigel, H. and Sigel, A. in Metal Ions in Biological Systems, N. D. Chasteen, Ed., Marcel Dekker, Inc., New York, 1995, vol. 31, p. 231-248.
107. Nechay, B. R., Nanninga, L. B., Nechay, P. S. E., *Arch. Biochem. Biophys.*, 1986, 251, 128-138.
108. Salmeen, A., Andersen, J., Myers, M., Meng, T., Hinks, J., Tonks, N., Bradford, D., *Nature*, 2003, 424, 769-773.
109. Cohen, M., Sisco, M., Prophete, C., Chen, L., Zelikoff, J. T., Ghio, A. J., Stonehuerner, J. D., Smee, J. J., Holder, A. A., Crans, D. C., *J. Immunotoxicol.*, 2007, 4, 49-60.
110. Wieghardt, K. *Inorg. Chem.* 1978, 17, 57-64.
111. Crans, D. C.; Yang, L.; Jakusch, T.; Kiss, T. *Inorg. Chem.* 2000, 39, 4409-4416.
112. Crans, D. C.; Rithner, C. D.; Baruah, B.; Gourley, B. L.; Levinger, N. E. *J. Am. Chem. Soc.* 2006, 128, 4437-4445.
113. Roess, D. A.; Smith, S. M. L.; Holder, A. A.; Baruah, B.; Trujillo, A. M.; Gilsdorf, D.; Stahla, M. L.; Crans, D. C. *ACS Symposium Series* 2007, 974, 121-134.
114. Cam, M. C.; Cros, G. H.; Serrano, J. J.; Lazaro, R.; McNeill, J. H. *Diabet. Res. Clinic. Pract.* 1993, 20, 111-121.
115. Goldwasser, I.; Li, J. P.; Gershonov, E.; Armoni, M.; Karnieli, E.; Fridkin, M.; Shechter, Y. *J. Biol. Chem.* 1999, 274, 26617-26624.
116. Al-qatati, A., Winter, P. W., Wolf-Ringwall, A. L., Chatterjee, P. B., Van Order, A. K., *Cell Biochem Biophys* 2012, 62:441-450.
117. Winter, P. W., Al-Qatati, A., Wolf-Ringwall, A. L., Schoeberl, S., Chatterjee, P. B., Barisas, B. G., Roess, D. A., Crans, D. C., *Dalton Trans.*, 2012, 41: 6419-6430.
118. Thompson, K. H. and Orvig, C., *Coor. Chem. Rev.* 2001, 219-221: 1033-1053.
119. Abdl-Khaegh Bordbar, A., Creagh L., Mohammadi, F., Haynes C. A., Orvig, C., *J. Inorg. Biochem.* 2009, 103, 643-647.
120. Lakowicz, J. R., Principles of Fluorescence Spectroscopy. Springer. Berlin, Germany, 2006, p353-412.
121. *Schematic of instrumentation for Time-correlated single photon counting anisotropy measurements*, Digital Image. Courtesy of Laura Swafford PhD, CSU, Fort Collins. 01 July 2009.

- 122 Prendergast, F. G., Haugland, R. P., Callahan, P. J., *Biochemistry* 1981, 20: 7333-7338.
- 123 Illinger, D., Poindron, P., Kuhry, J.-G., *Biol Cell* 1991, 71: 293-296.
- 124 Kuhry, J.-G., Duportail, G., Bronner, C., Laustriat, G., *Biochimica et Biophysica Acta* 1985, 845: 60-67.
- 125 Ribeiro, M. M. B., Domingues, M. M., Freire, J. M., Santos, N. C., Castanho, M. A. R. B. *Frontiers in Cellular Neuroscience*. 2012, 6: 1-7.
- 126 Xu, R. and Pecht, I. *Eur. J. Immunol.*, 2001, 31: 1571-1581.
- 127 Hemmerich, S. and Pecht, I. *Biochemistry*, 1988, 27: 7488-7498.
- 128 Rahman, N. A., Pecht, I., Roess, D. A., Barisas, B. G., *Biophys. J.*, 1992, 61: 334-346.
- 129 Abramson, J. and Pecht, I. *Immunol. Lett.*, 2002, 82: 23-28.
- 130 Andrews, N. J., Pfeiffer, J. R., Martinez, A. M., Haaland, D. M., Davis, R. W., Kawakami, T., Oliver, J. M., Wilson, B. S., Lidke, D. S., *Immunity*, 2009, 31: 469-479.
- 131 McNeill, J. H., Yuen, V. G., Hoveyda, H. R., Orvig, C., *Journal of Medical Chemistry* 1992, 35: 1489-1491.
- 132 Orvig, C., McNeill, J. H., Vasilevskis, J., Metal Ions in Biological Systems, Sigel, H. and Sigel, A., Eds., Marcel Dekker, Inc., New York 1995, p. 575-594.
- 133 Pasquali R., Gambineri A., Anconetani B., Vicennati V., Colitta D., Caramelli E., Casimirri F., Morselli-Labate, A. M., *Clin Endocrinol (Oxf)*. 1999, 50: (4):517.

## LIST OF ABBREVIATIONS

3T3-L1:	cell line of adipocytes
Akt:	serine/threonine specific kinase, also known as PKB
APS:	Cbl binding protein
BEOV:	bis(ethylmaltolato)oxovanadium (IV) complex
BMOV:	bis(maltolato)oxovanadium(IV) complex
C3G:	guanine nucleotide exchange factor
CAP :	cyclase associated protein
c-Cbl:	E3 ubiquitin-protein ligase adaptor molecule
CDase:	ceramidase
DAG	diacylglycerol
EDTA:	ethylenediamine tetraacetic acid
FABP:	fatty acid binding protein
Fas:	cell surface receptor which signals cell death
FBS:	fetal bovine serum
FFA:	free fatty acid
FKHR:	transcription factor “forkhead in human rhabdomyosarcoma” (FOXO1a)
FSH:	follicle stimulating hormone
GLUT4:	glucose transporter 4
GM-3:	a subset of ganglioside
GPx :	glutathione peroxidase
GSK3:	glycogen synthase kinase 3, a serine threonine kinase
HDL:	high density lipoprotein

IBH:	fluorometer manufactured by Jovin Horiba
IGF-1:	insulin-like growth factor-1
IGF-2	insulin-like growth factor-2
IKK $\beta$ :	inhibitor of nuclear factor kappa-B kinase
IR:	insulin receptor
IRS-1:	insulin receptor substrate 1
JNK:	c-Jun N-terminal kinase
LDL:	low density lipoprotein
LH:	luteinizing hormone
LO:	liquid ordered
MD:	microdomain
MEM:	Minimum Essential Medium
mRNA:	messenger ribonucleic acid
NEFA:	non-esterified fatty acid
NF $\kappa$ B:	nuclear factor kappa-light-chain-enhancer of activated B cells
OS:	oxidative stress
PI3K:	phosphatidylinositol 3-kinase
P70S6K:	p70 ribosomal S6 kinase
PBS:	phosphate buffered saline
PC:	phosphatidylcholine
PCOS:	polycystic ovarian syndrome
PE	phosphatidylethanolamine
PIP2:	phosphatidylinositol-4 5-bisphosphate

PIP3:	phosphatidylinositol (3,4,5)-triphosphate
PKB:	protein kinase B
PKC:	protein kinase C
PM:	plasma membrane
PP1:	protein phosphatase 1 (class of serine/threonine phosphatase)
PPAR:	peroxisome proliferator-activated receptors
PS:	phosphatidylserine
PSA:	penicillin + streptomycin + amphotericin B
PTPase:	protein tyrosine phosphatase
Rac:	subset of Rho family GTPases
RBL-2H3:	rat basophilic leukemia cell line
RNA:	ribonucleic acid
RNS:	reactive nitrogen species
ROS:	reactive oxygen species
S1P	sphingosine 1-phosphate
Ser:	serine
SER:	smooth endoplasmic reticulum
SH2:	Src homology 2 domain
Shc:	Src homology domain containing
SHIP2:	SH2 domain containing inositol 5-phosphatase 2
SM:	sphingomyelin
SMase:	sphingomyelinase
SREBP-1:	Sterol regulatory element-binding protein-1

TC10: protein member of Rho family of GTPases  
TG: triglyceride  
Thr: threonine  
TMA-DPH: 1-(4-trimethylammoniumphenyl)-6-phenyl-1,3,5-hexatriene p-toluenesulfonate  
TNF- $\alpha$ : tumor necrosis factor-alpha  
VO<sub>2</sub>dipic: dipicolinatooxovanadium(V)